

# Attribution of Seasonal Climate Anomalies

## April-May-June 2019

# Summary of April-May-June 2019 Observed Conditions and Outlooks

- Weak Central Pacific El Niño sea surface temperature (SST) conditions in observations (slide 9).
- Consistent with El Niño conditions, above normal Tropical 200-mb height and above normal rainfall near the dateline in observations (slide 10); these were well captured by model simulations and initialized forecasts (slides 15 & 16).
- Over North America, there was some resemblance in 200-mb height response in AMIP simulations (slide 20). This is also apparent in the distribution of correlations between observations and individual AMIP simulations (slide 24).
- After a series of consecutive negative skill scores during winter/spring of 2018-19 for the forecast of seasonal mean surface temperature over the US, forecast skill returned to positive territory.

# Attribution of Seasonal Climate Anomalies

- Goal
  - In the context of prediction of seasonal climate variability, utilize seasonal climate forecasts and atmospheric general circulation model (AGCM) simulations to attribute possible causes for the observed seasonal climate anomalies.
  - The analysis can also be considered as an analysis of predictability of the observed seasonal climate anomalies.

# Outline

- Methodology
- Data description
- Observed seasonal anomalies
- Ensemble mean seasonal mean anomalies from AGCM simulations and initialized forecasts
- Seasonal mean anomalies from the individual AGCM simulations and initialized forecasts
- References

# Methodology - 1

- Compare observed seasonal mean anomalies with those from model simulations and forecasts.
- Ensemble averaged model simulated/predicted seasonal mean anomalies are an indication of the predictable (or attributable) component of the corresponding observed anomalies.
- For seasonal mean atmospheric anomalies, predictability could be due to
  - Anomalous boundary forcings [e.g., sea surface temperature (SSTs); soil moisture etc.];
  - Atmospheric initial conditions.
- The influence of anomalous boundary forcings (particularly due to SSTs, can be inferred from the ensemble mean of AGCM simulations forced by observed SSTs, the so called AMIP simulations). This component of predictability (or attributability) is more relevant for longer lead seasonal forecasts.

## Methodology - 2

- The influence of the atmospheric initial state can be inferred from initialized predictions. This component is more relevant for short lead seasonal forecasts.
- The influence of unpredictable component in the atmospheric variability can be assessed from the analysis of individual model simulations, and the extent anomalies in individual runs deviate from the ensemble mean anomalies.
- The relative amplitude of ensemble averaged seasonal mean anomalies to the deviations of seasonal mean anomalies in the individual model runs from the ensemble average is a measure of seasonal predictability (or the extent observed anomalies are attributable).
- Observed anomalies are equivalent to a realization of a single model run, and therefore, analysis of individual model runs also gives an appreciation of how much observed anomalies can deviate from the component that is attributable (Kumar et al. 2013).

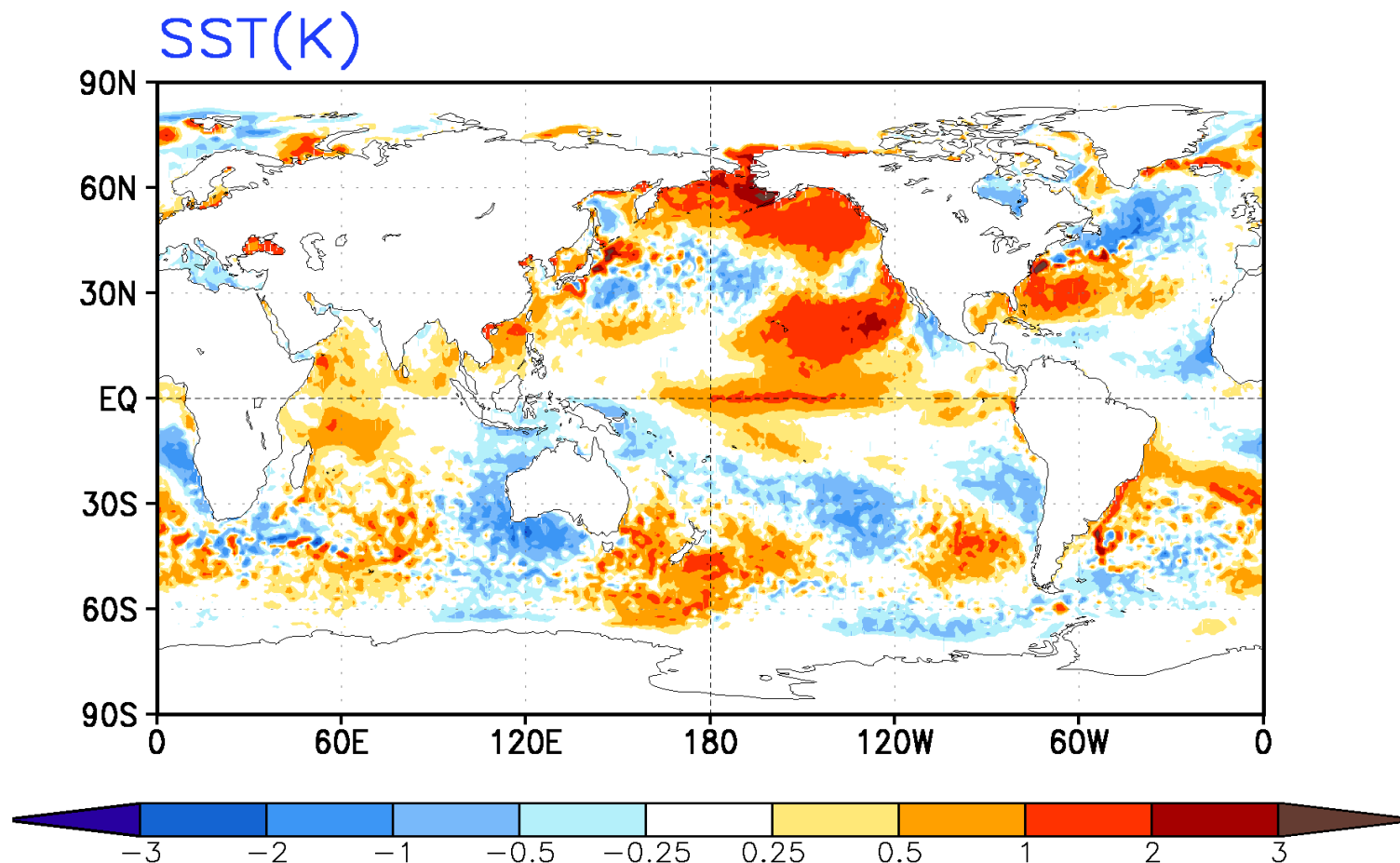
# Data

- Observations
  - SST: NCDC daily OI analysis (Reynolds et al., 2007)
  - Prec: CMAP monthly analysis (Xie and Arkin, 1997)
  - T2m: GHCN-CAMS land surface temperature monthly analysis (Fan and van den Dool, 2008)
  - 200mb height (z200): CFSR (Saha et al., 2010)
- 0-month-lead seasonal mean forecasts from CFSv2 (Saha et al. 2014)
  - Seasonal forecast: the seasonal mean forecasts based on 40 members from the latest 10 days before the target season (0-month-lead);
  - Reconstructed forecast: the seasonal mean forecasts constructed from 3 individual monthly forecasts with the latest 10 days initial conditions for each individual monthly forecasts. This approach for constructing seasonal mean anomalies has more influence from the initial conditions (Kumar et al. 2013);
- Seasonal mean AMIP simulation from CFSv2 (provided by Dr. Bhaskar Jha)
  - 18 members
- All above seasonal mean anomalies are based on 1999-2010 climatology.
- z200 responses to tropical heating in linear model (provided by Dr. Peitao Peng)
- Seasonal mean anomalies of z200, T2m, and Prec forecasted from the Constructed Analog Model (provided by Dr. Peitao Peng)

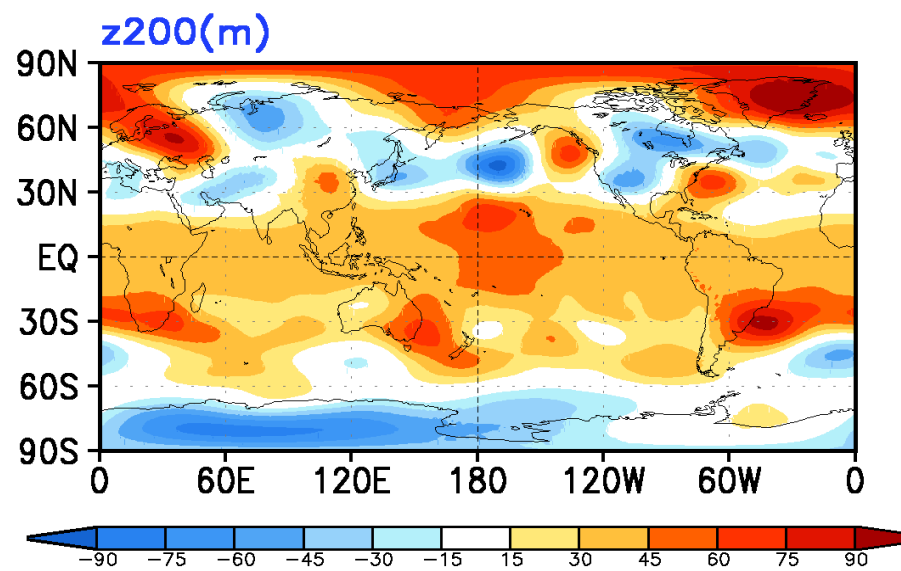
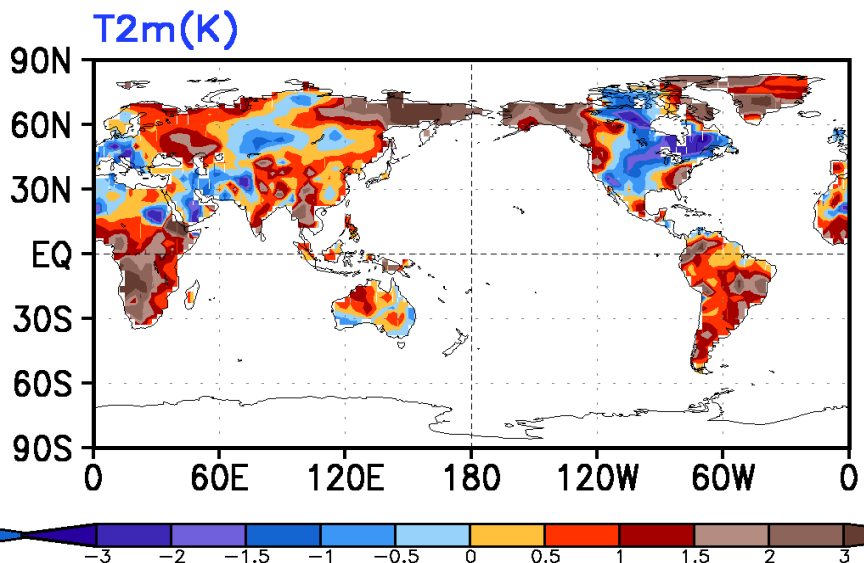
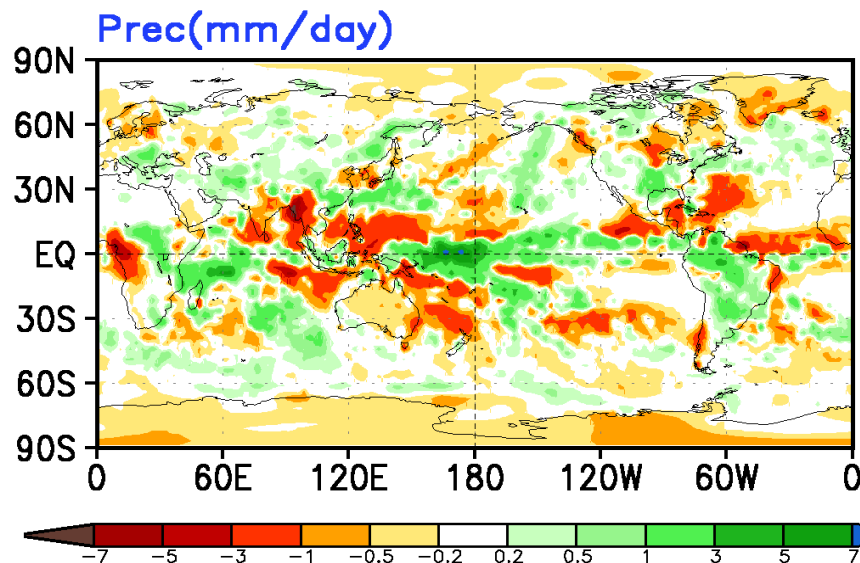
# Observed Seasonal Anomalies

## Global and North America

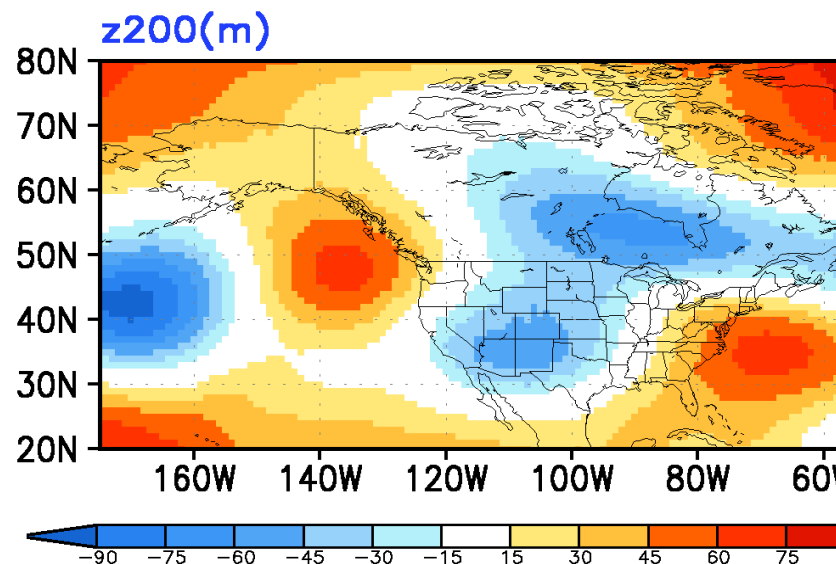
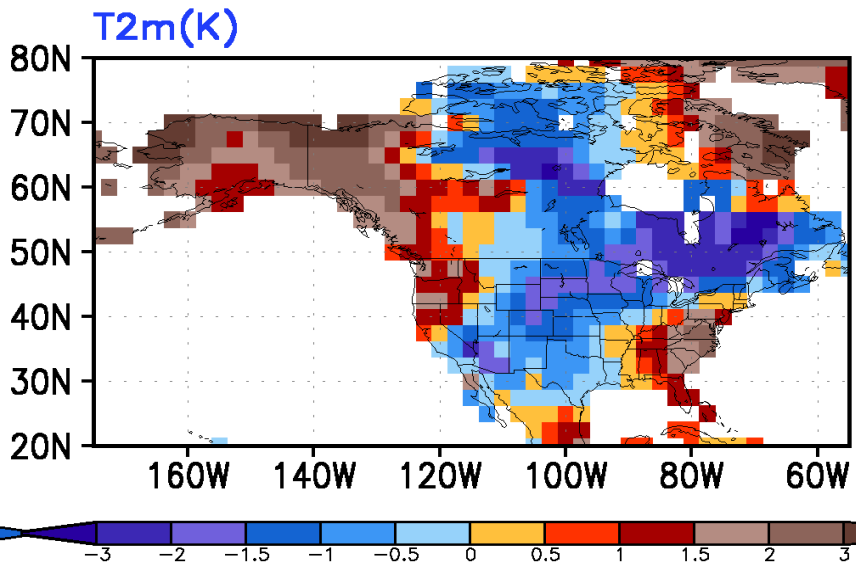
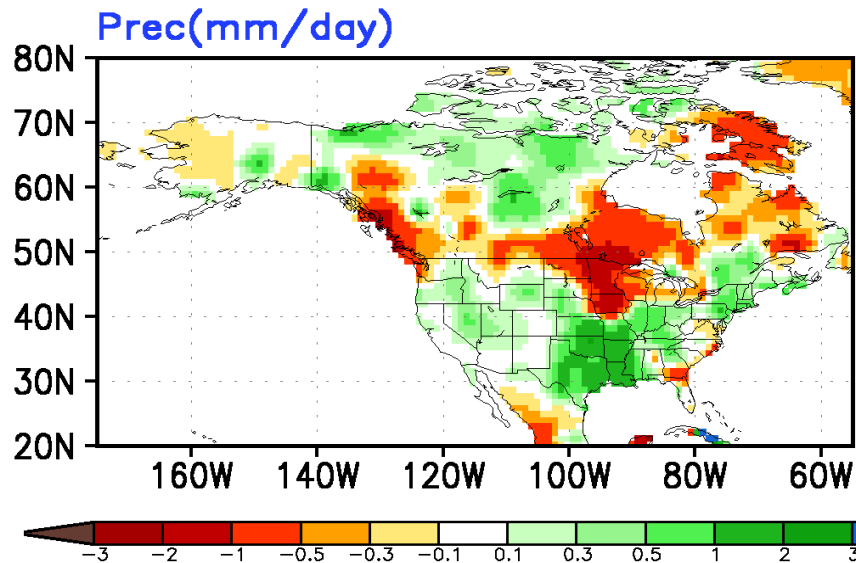
# Observed Anomaly AMJ2019



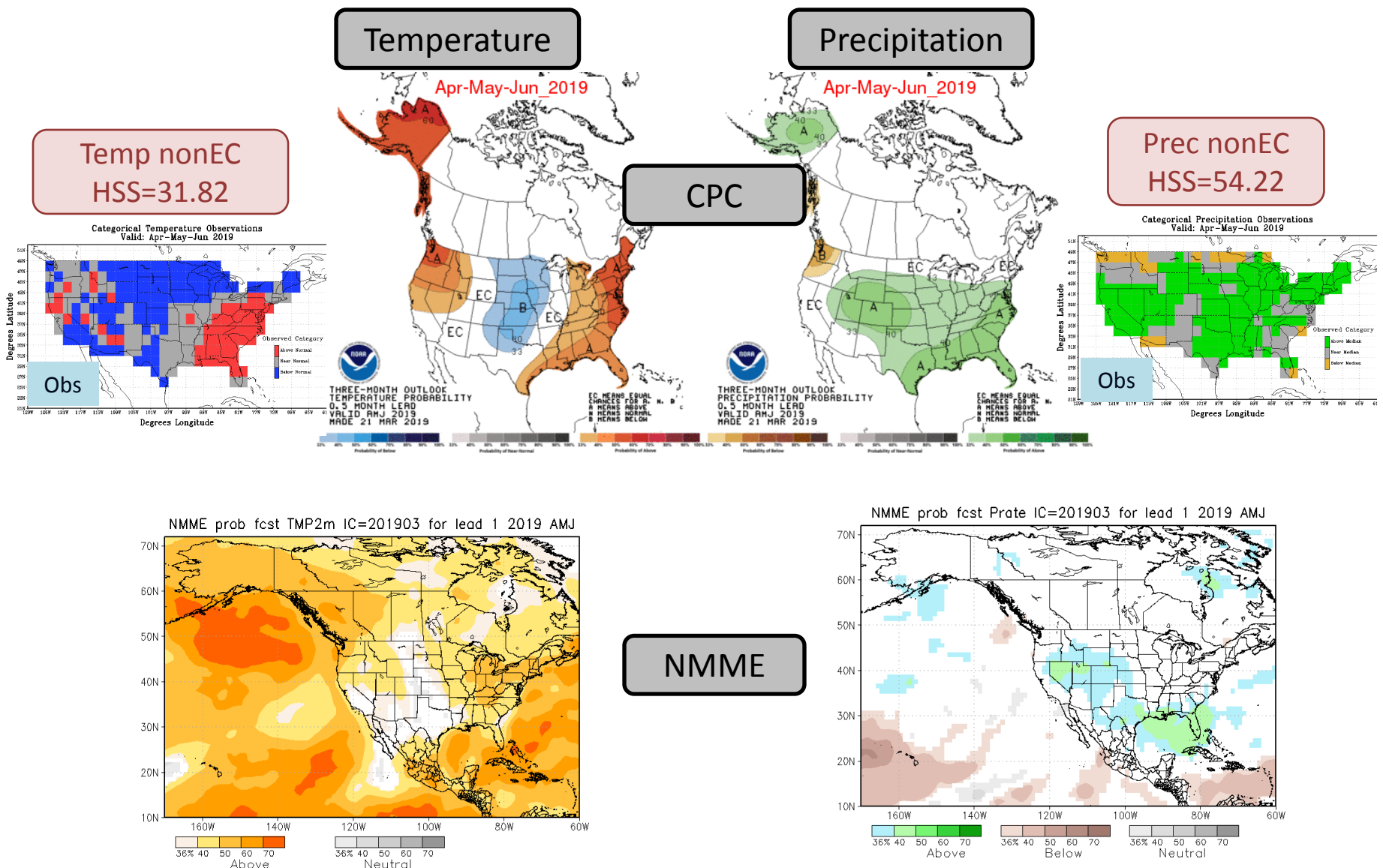
# Observed Anomaly AMJ2019



# Observed Anomaly AMJ2019



# AMJ2019 CPC Seasonal Outlooks and NMME Forecasts

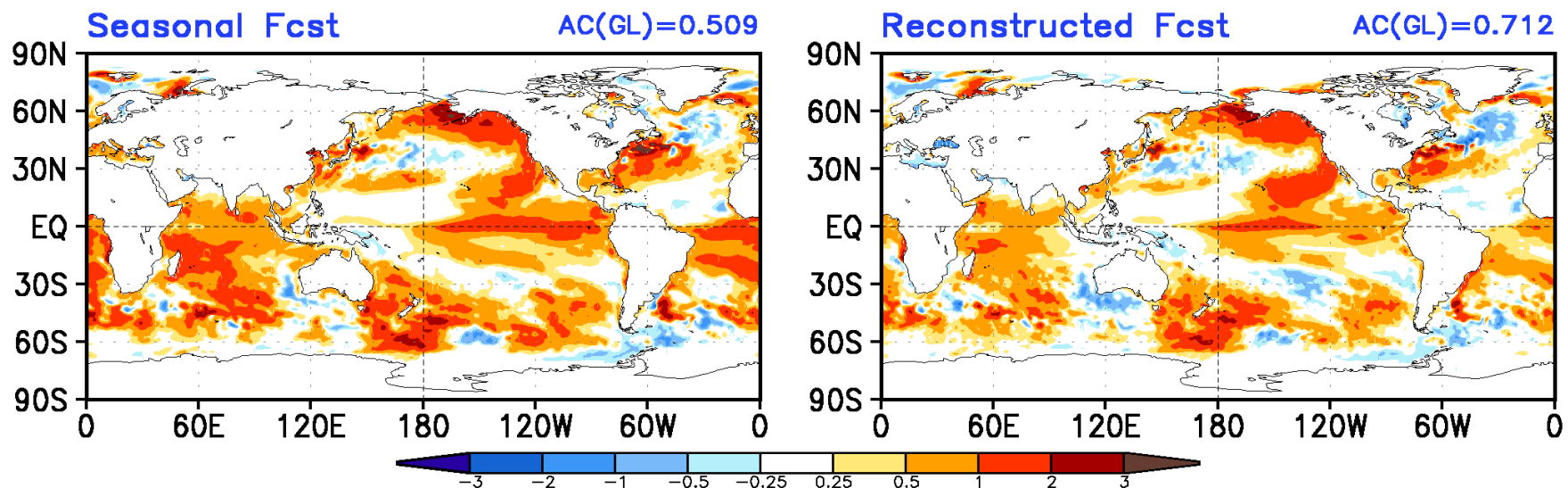
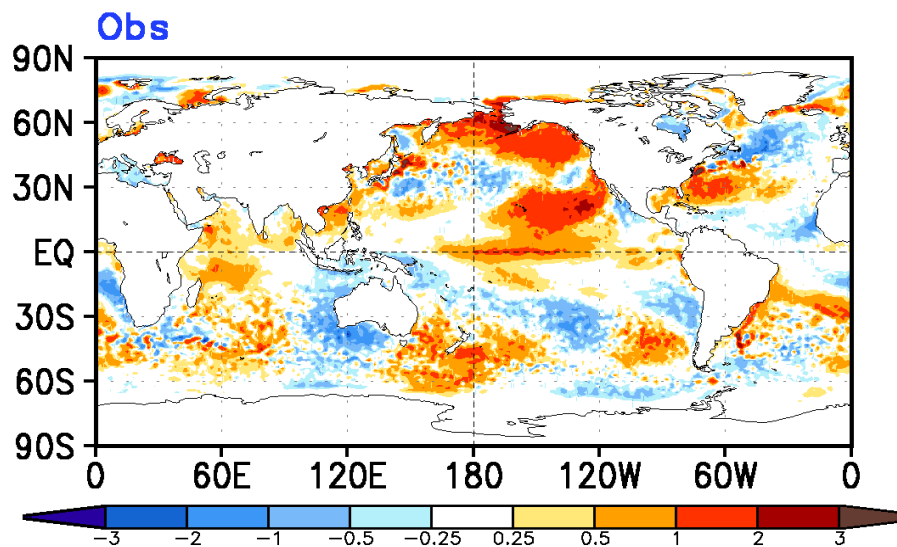


## Model Simulated/Forecast Ensemble Mean Anomalies

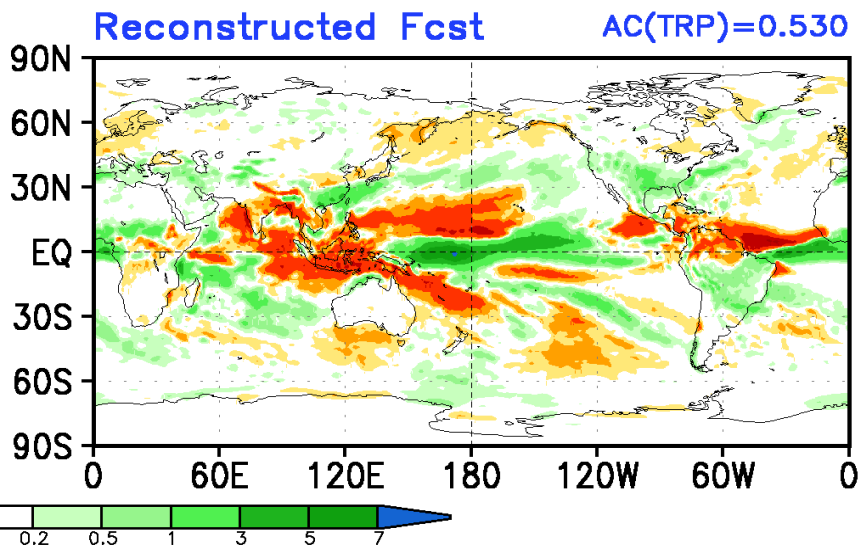
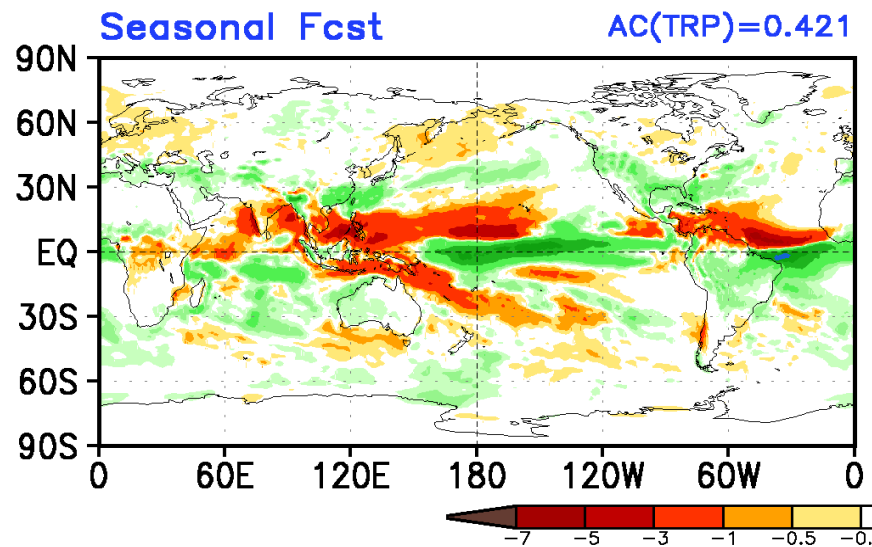
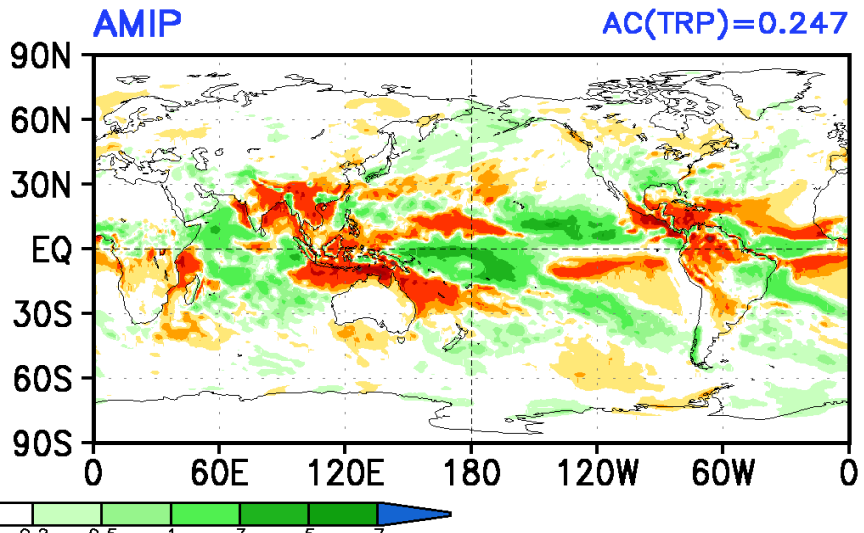
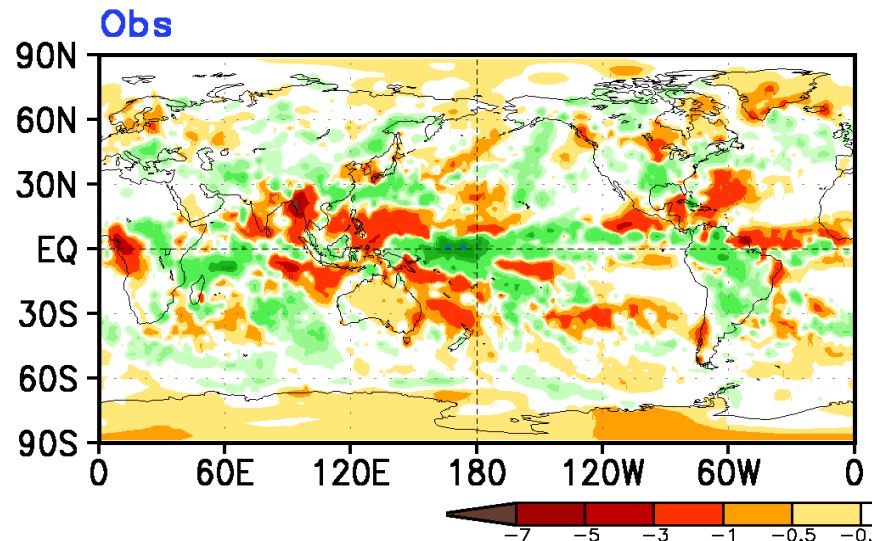
# Model Simulated/Forecast Ensemble Average Anomalies

- CFS **AMIP simulations** forced with observed sea surface temperatures (18 members ensemble)
- CFSv2 real time operational forecasts
  - Seasonal forecast: the seasonal mean forecasts based on 40 members from the latest 10 days before the target season (0-month-lead). For example, 2016AMJ seasonal mean forecasts are 40 members from 22-31 March2016 initial conditions.
  - Reconstructed forecast: the seasonal mean forecasts constructed from 3 individual monthly forecasts with the latest 10 days initial conditions for each individual monthly forecasts. This approach for constructing seasonal mean anomalies has more influence from the initial conditions (Kumar et al. 2013). For example, the constructed 2016AMJ seasonal mean forecasts are the average of April2016 forecasts from 22-31 March2016 initial conditions, May2016 forecasts from 21-30 April2016 initial conditions, and June2016 forecasts from 22-31 May2016 initial conditions.
- Numbers at the panels indicate the spatial anomaly correlation (AC).

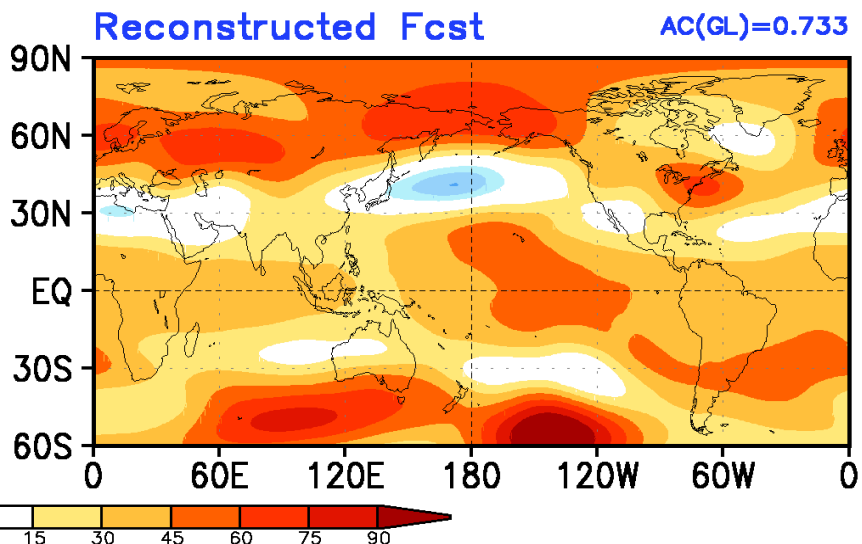
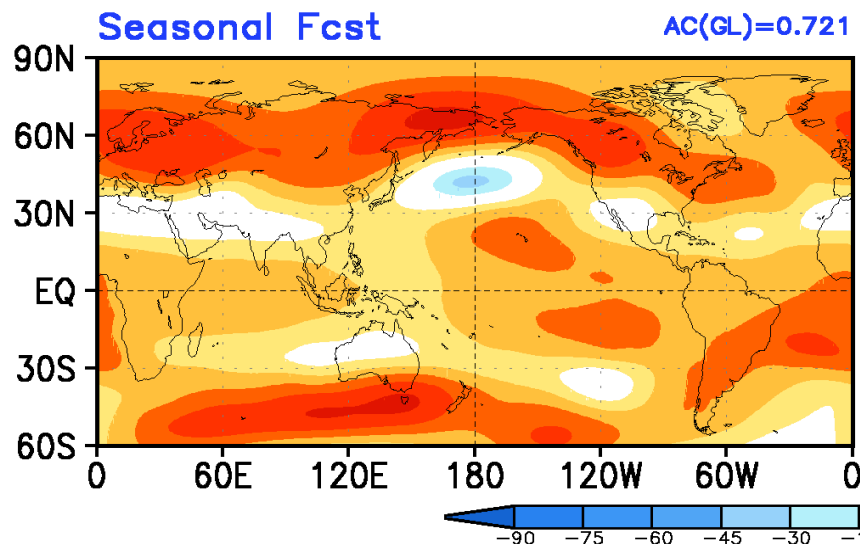
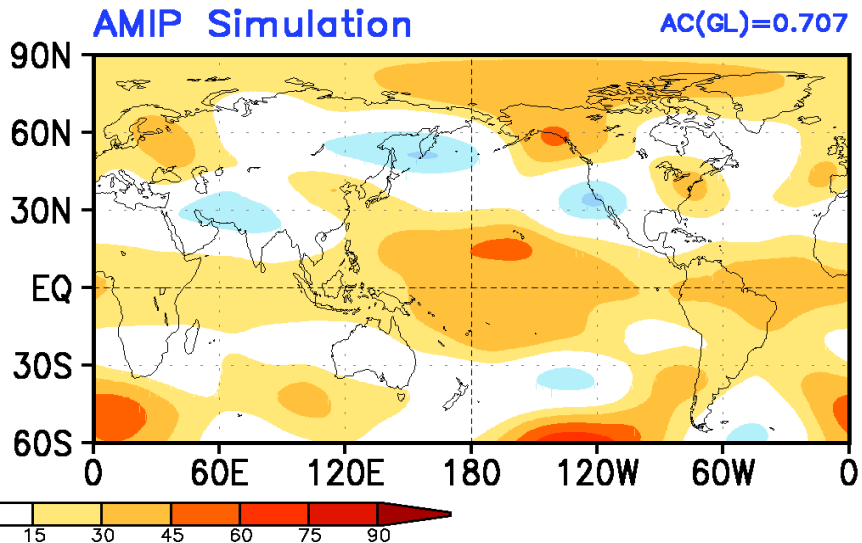
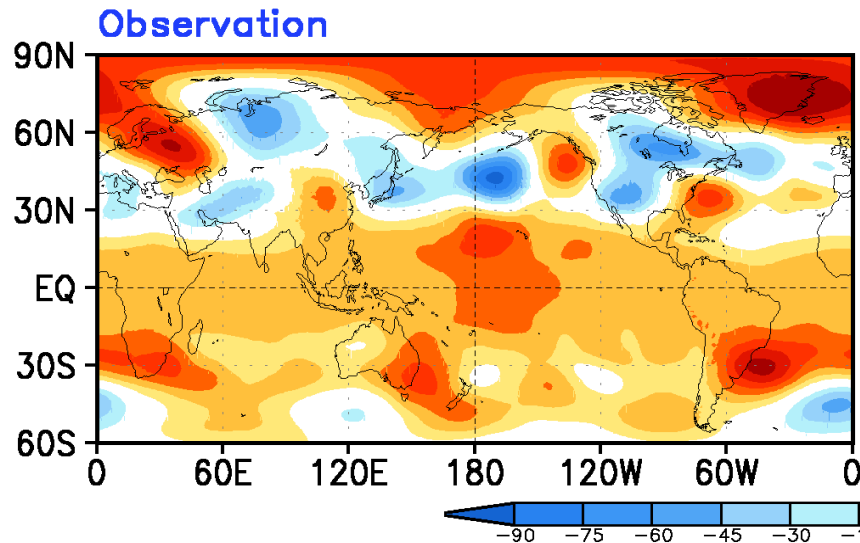
# AMJ2019 Observed & Model Simulated/Forecast Ensemble Average Anomalies SST(K)



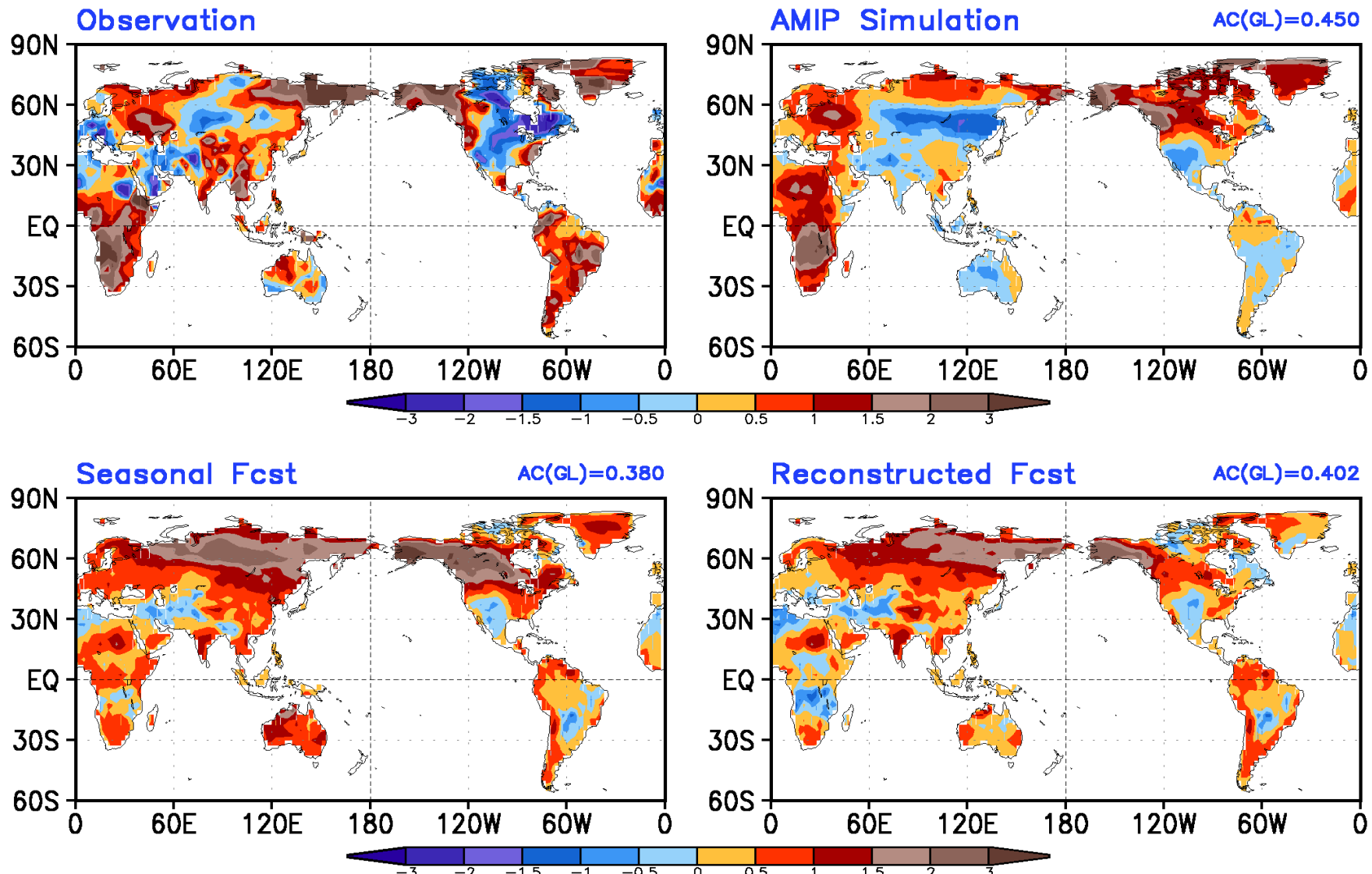
# AMJ2019 Observed & Model Simulated/Forecast Ensemble Average Anomalies Prec(mm/day)



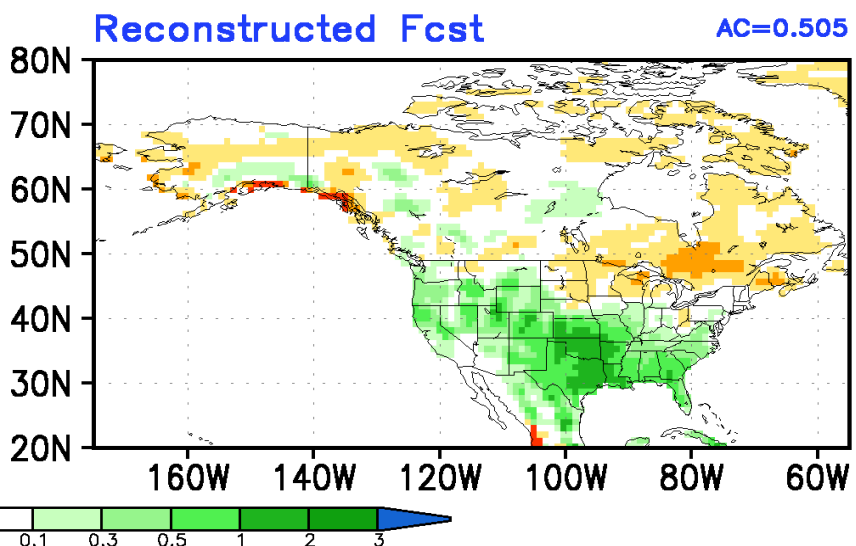
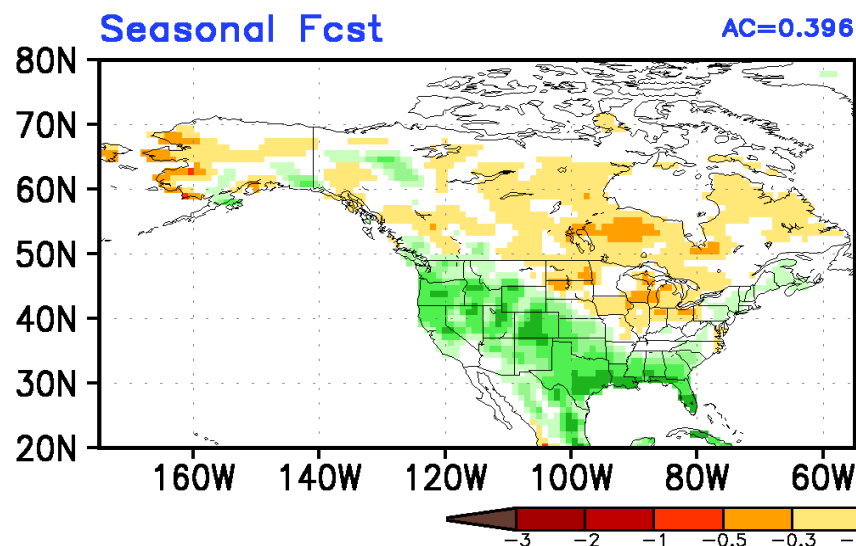
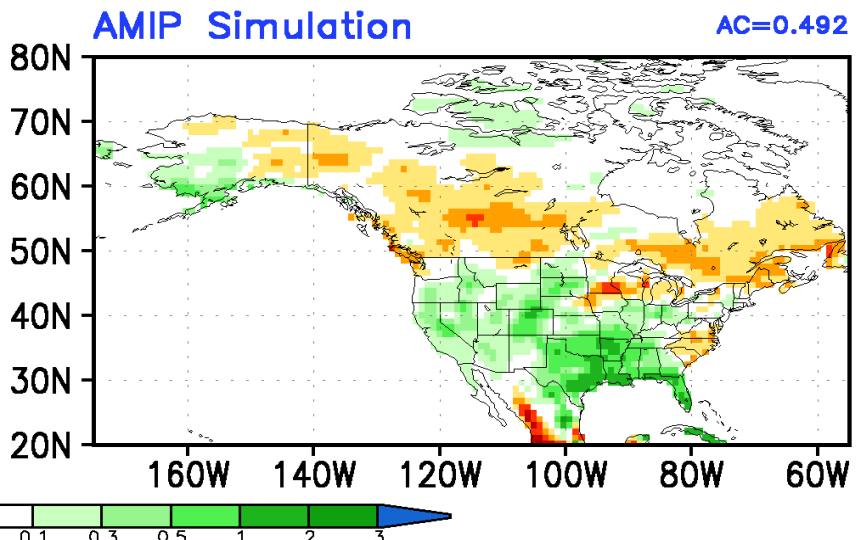
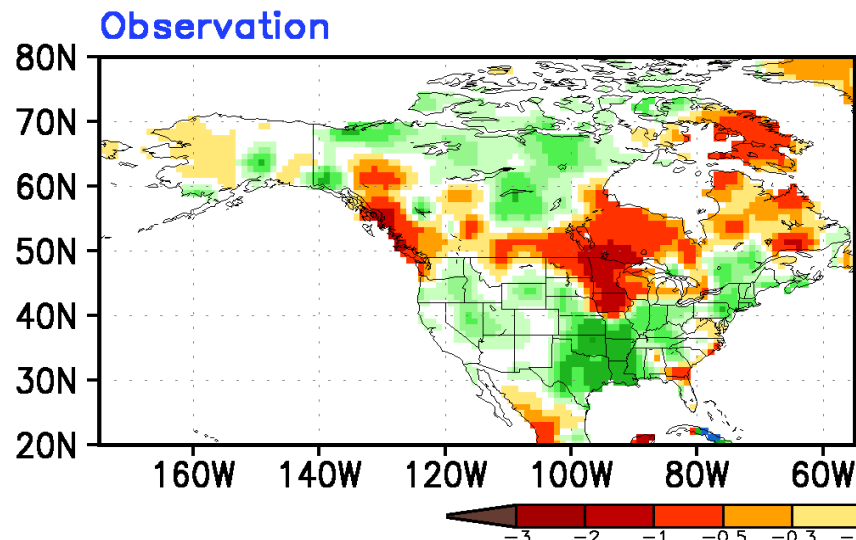
# AMJ2019 Observed & Model Simulated/Forecast Ensemble Average Anomalies z200(m)



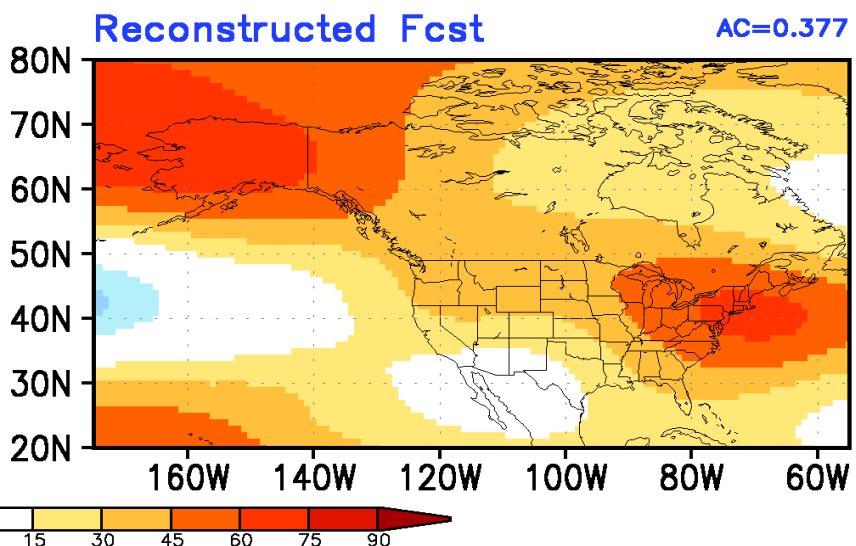
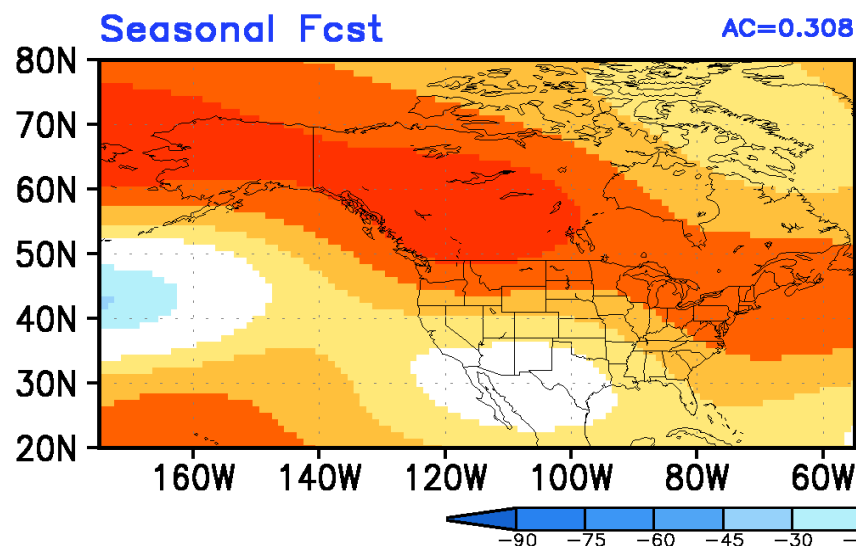
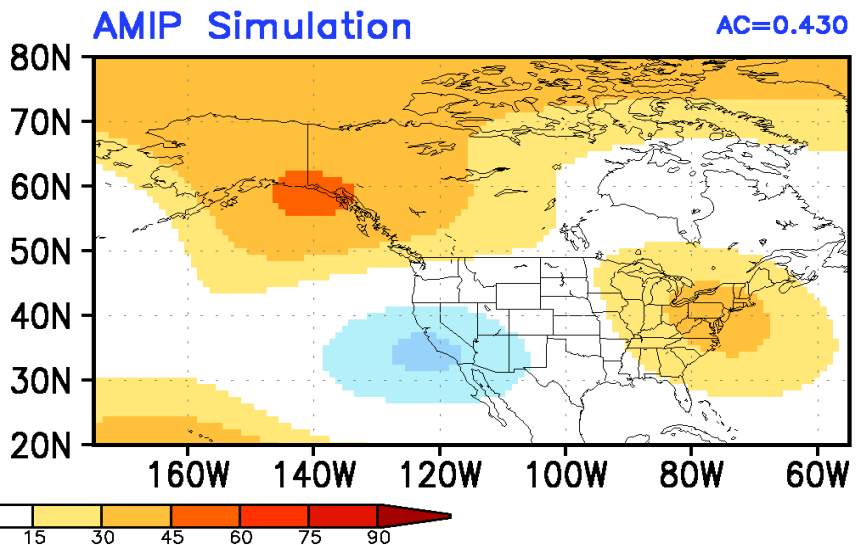
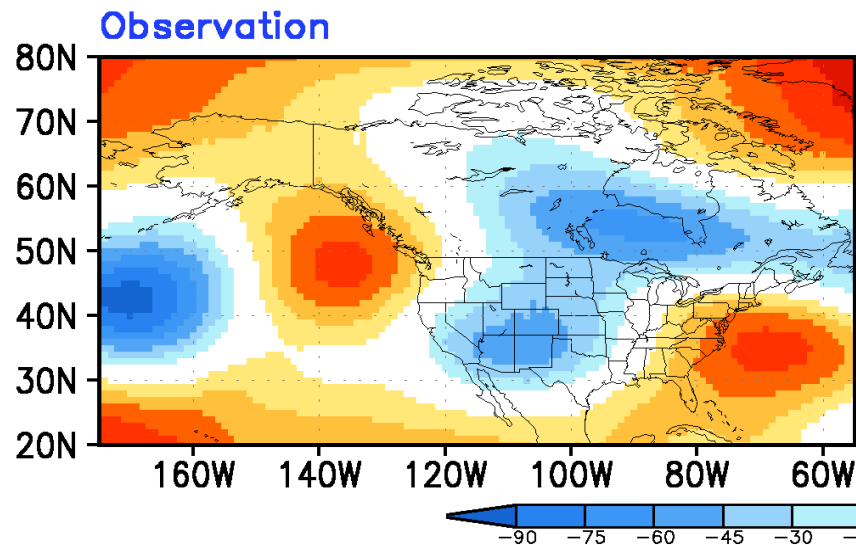
# AMJ2019 Observed & Model Simulated/Forecast Ensemble Average Anomalies T2m(K)



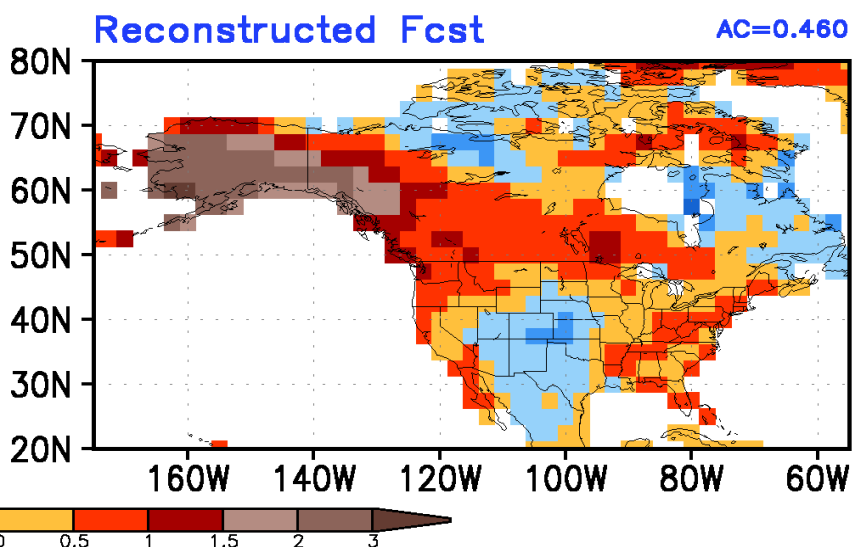
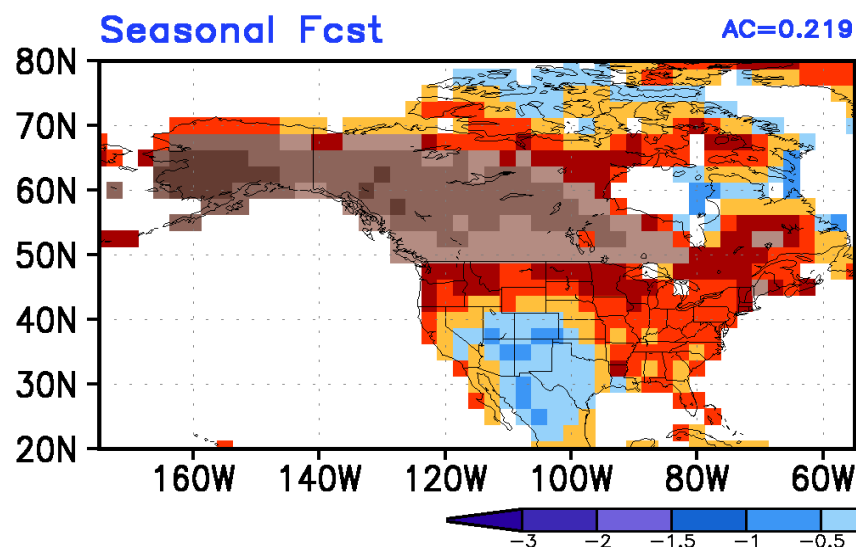
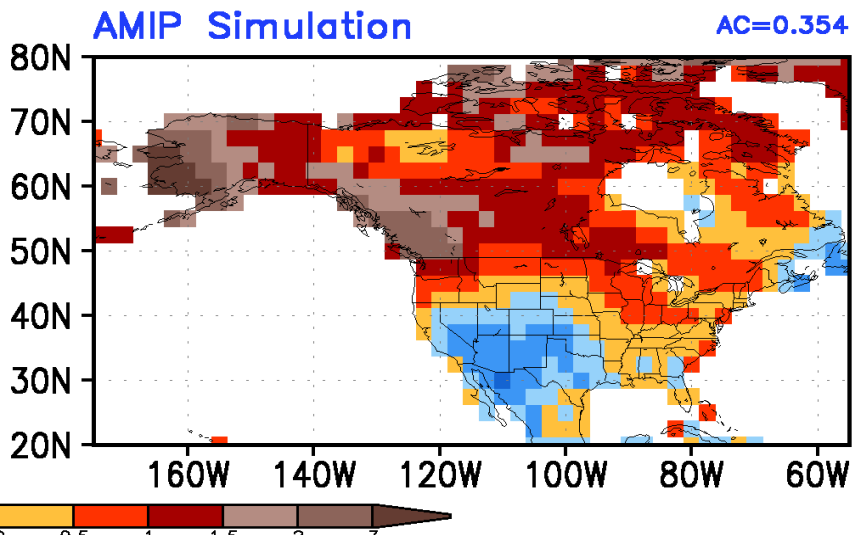
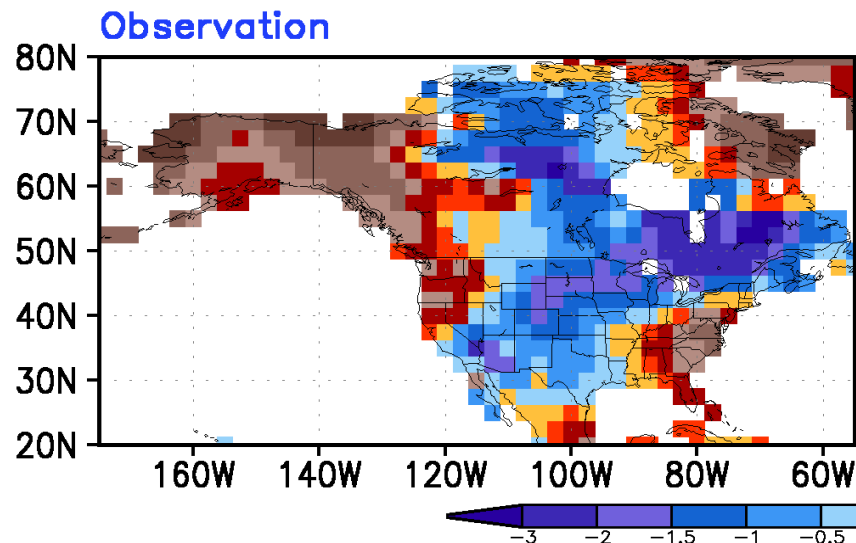
# AMJ2019 Observed & Model Simulated/Forecast Ensemble Average Anomalies Prec(mm/day)



# AMJ2019 Observed & Model Simulated/Forecast Ensemble Average Anomalies z200(m)



# AMJ2019 Observed & Model Simulated/Forecast Ensemble Average Anomalies T2m(K)

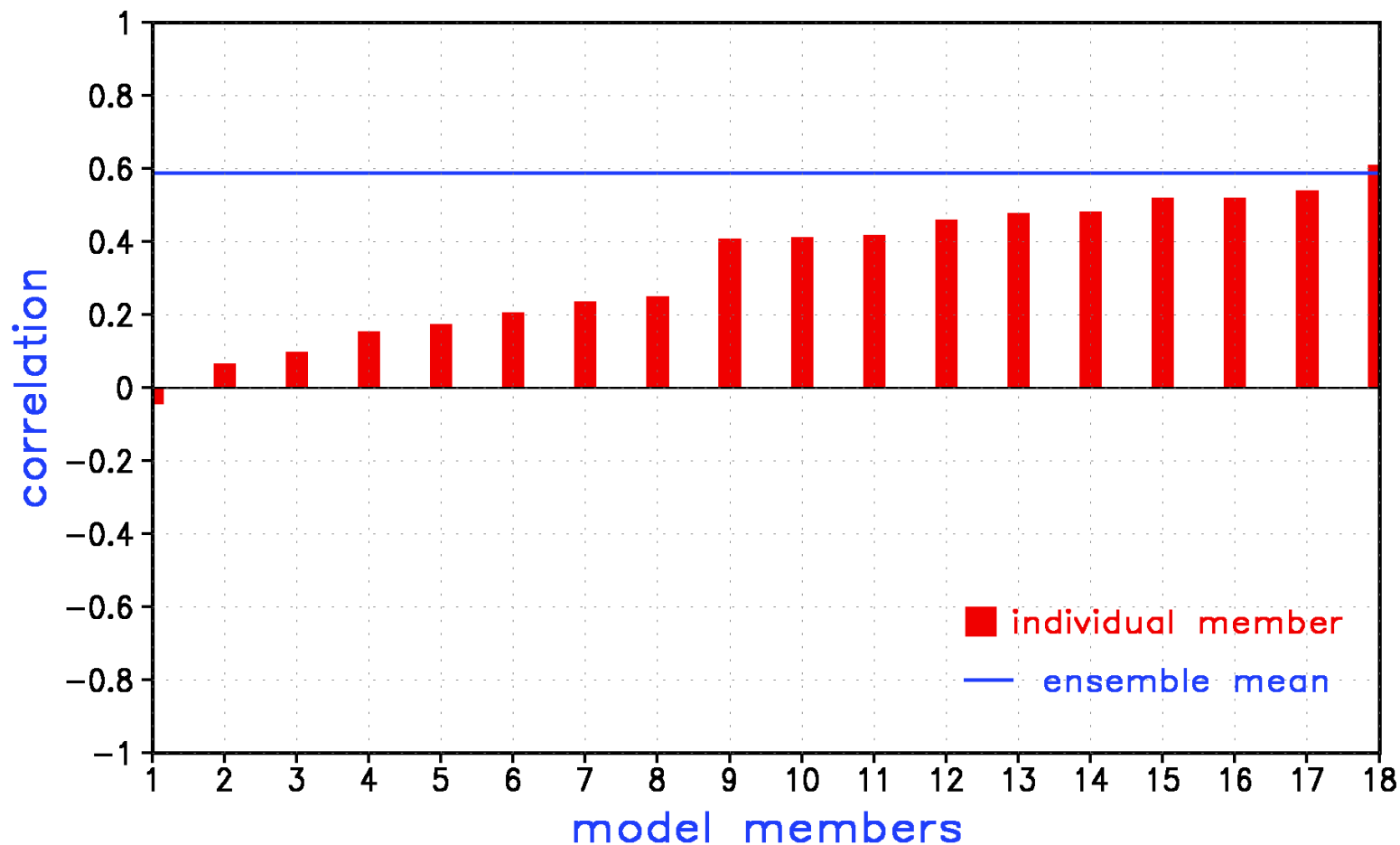


# Model Simulated/Forecast Anomalies: Individual Runs

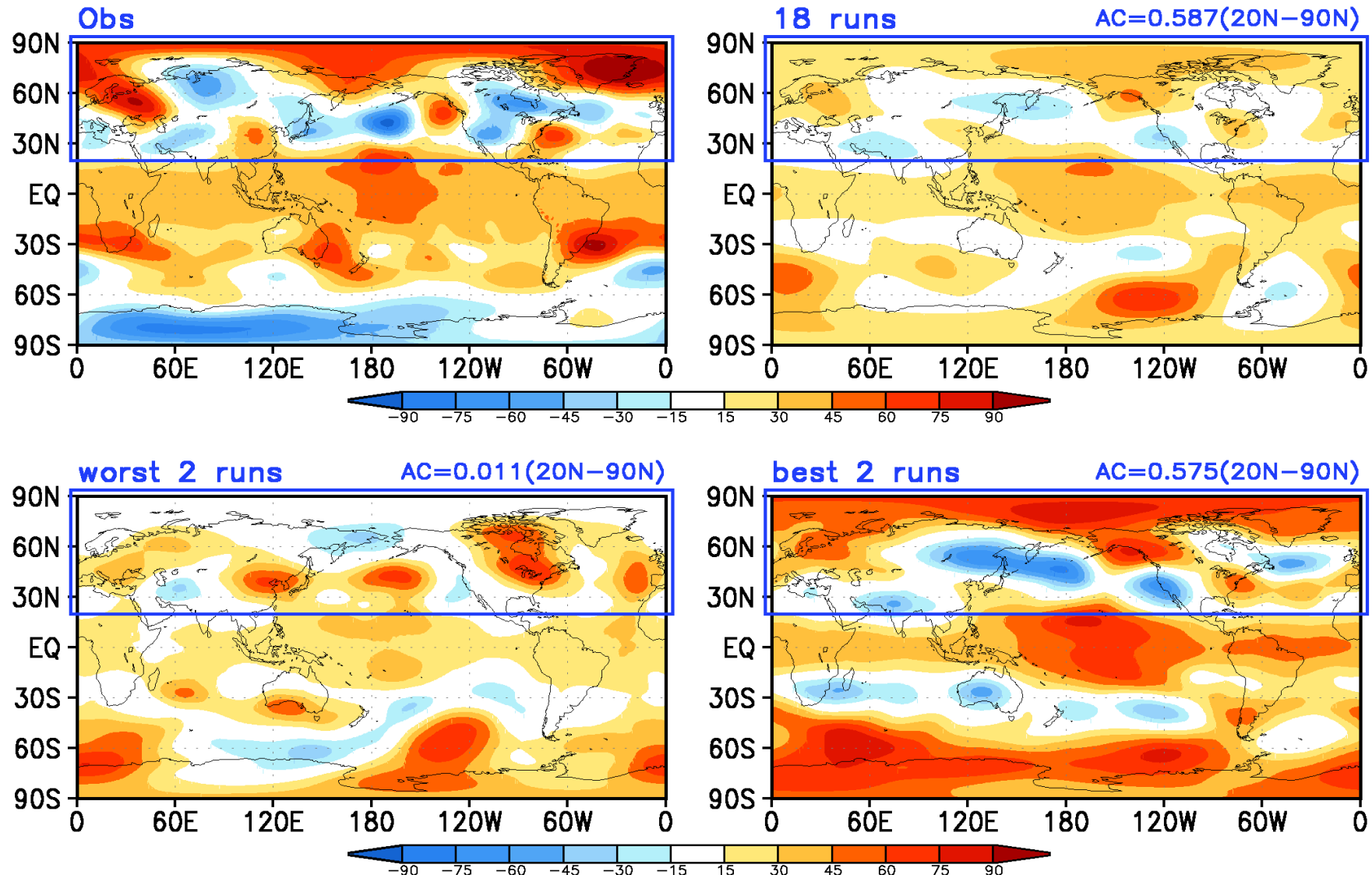
# Model Simulated/Forecast Anomalies: Individual Runs

- In this analysis, anomalies from individual model runs are compared against the observed seasonal mean anomalies. The spatial resemblance between them is quantified based on anomaly correlation (AC).
- The distribution of AC across all model simulations is indicative of probability of observed anomalies to have a predictable (or attributable) component.
- One can also look at best and worst match between model simulated/forecast anomalies to assess the range of possible seasonal mean outcomes.

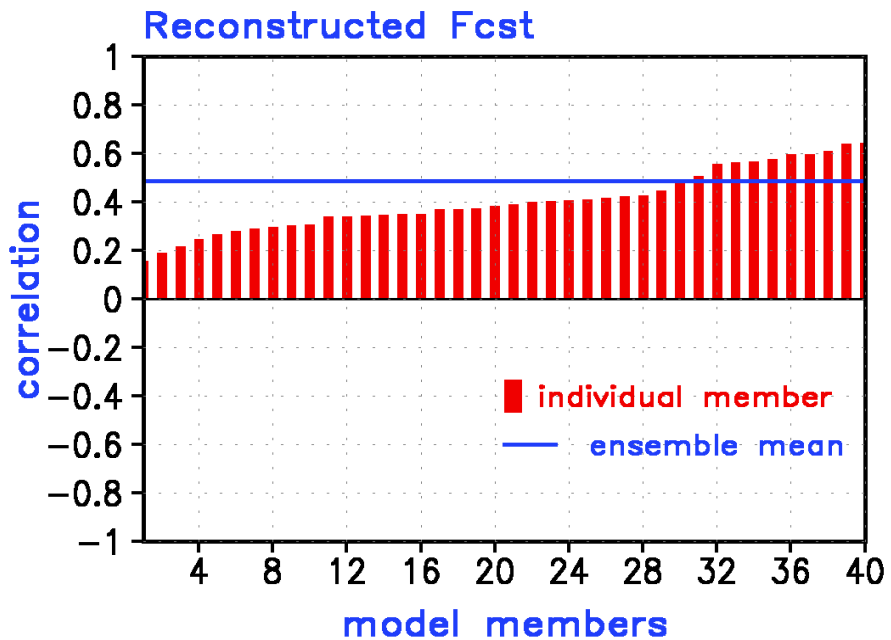
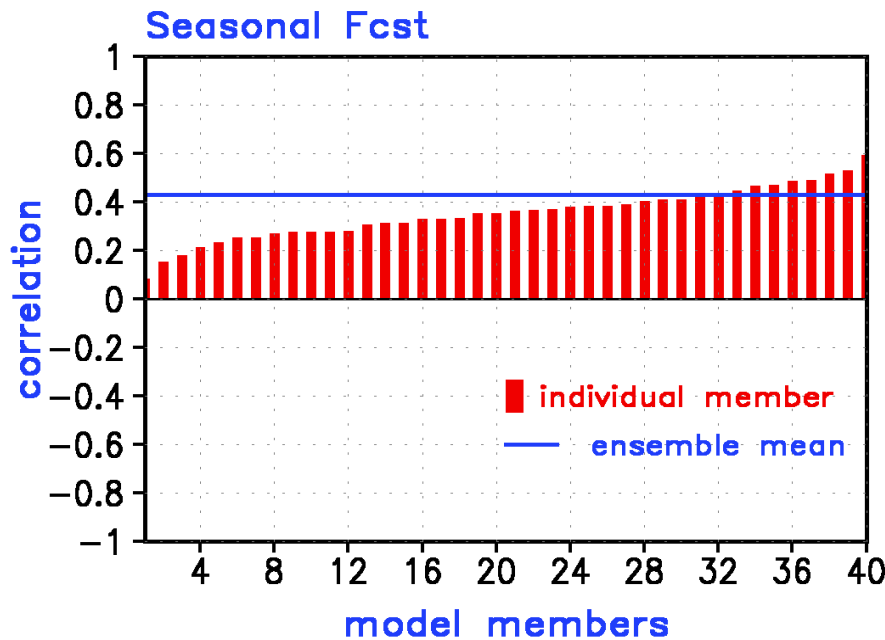
# AMJ2019 Anomaly Correlation for Individual AMIP Simulation with Observation -- z200(20N–90N)



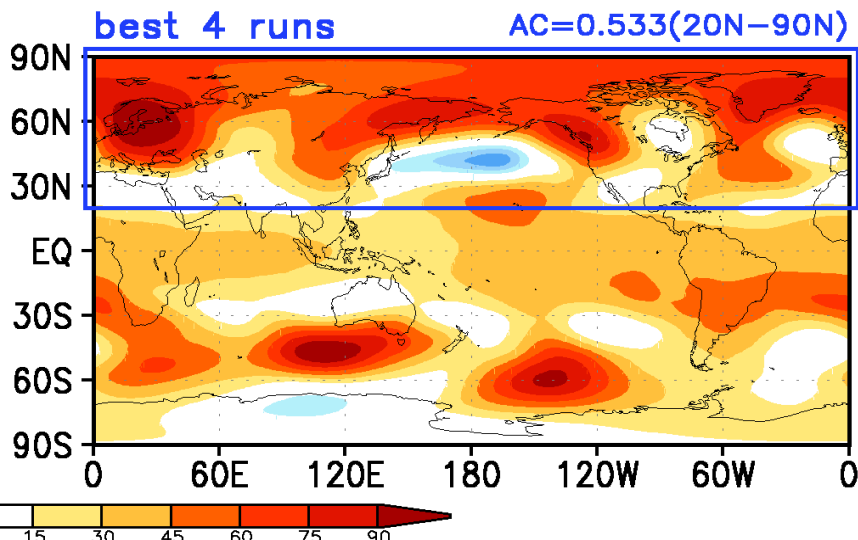
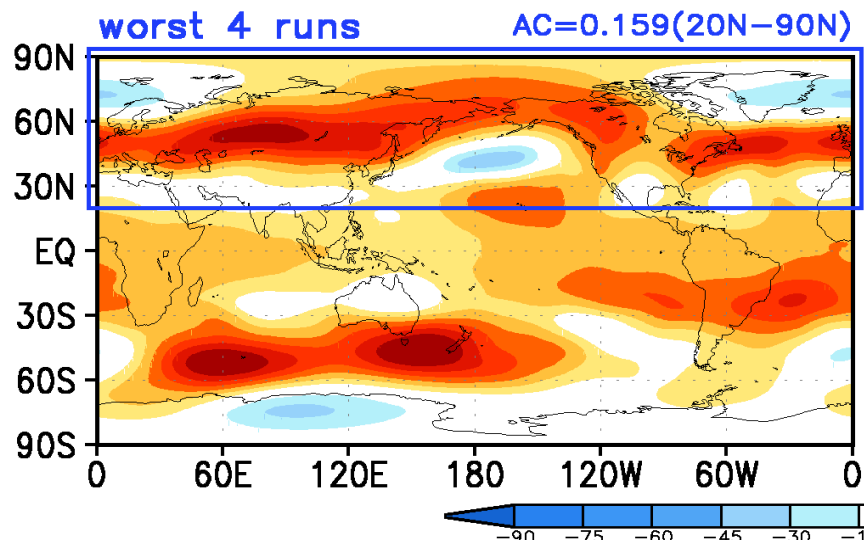
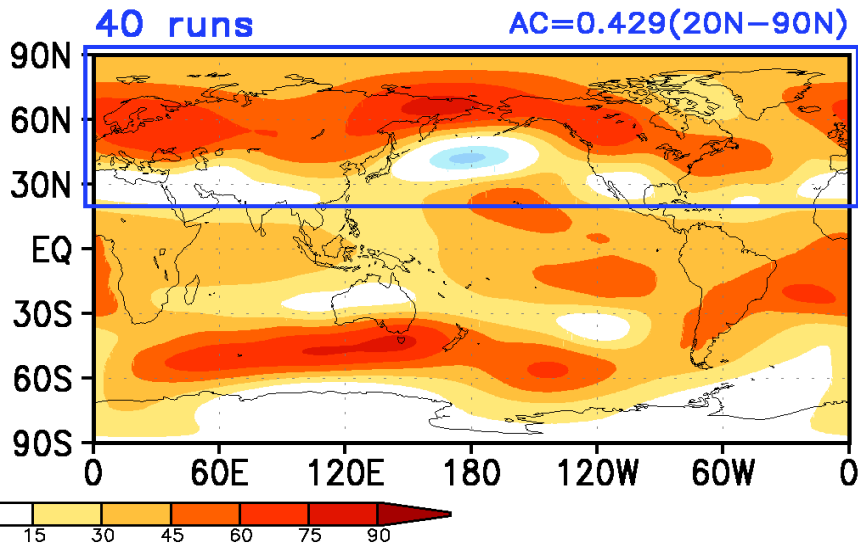
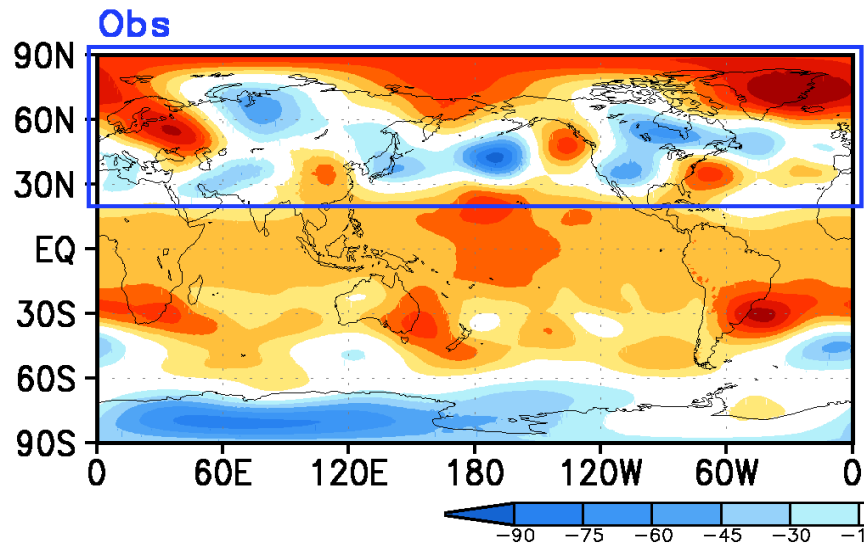
Observed & AMIP Ensemble Average Anomalies  
AMJ2019 z200(m) 18 runs/worst 2 runs/best 2 runs



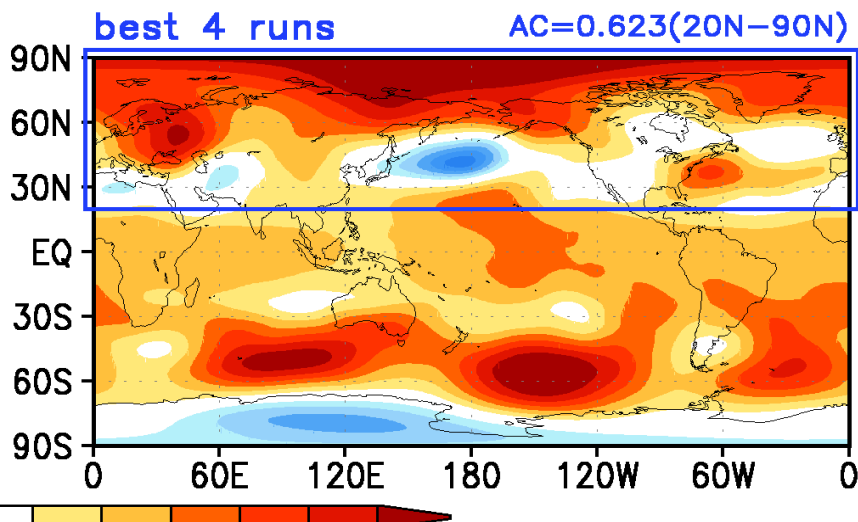
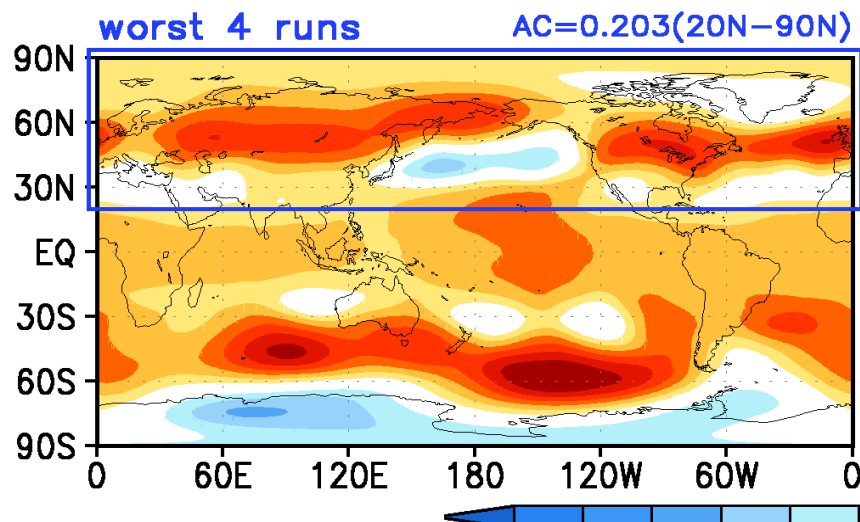
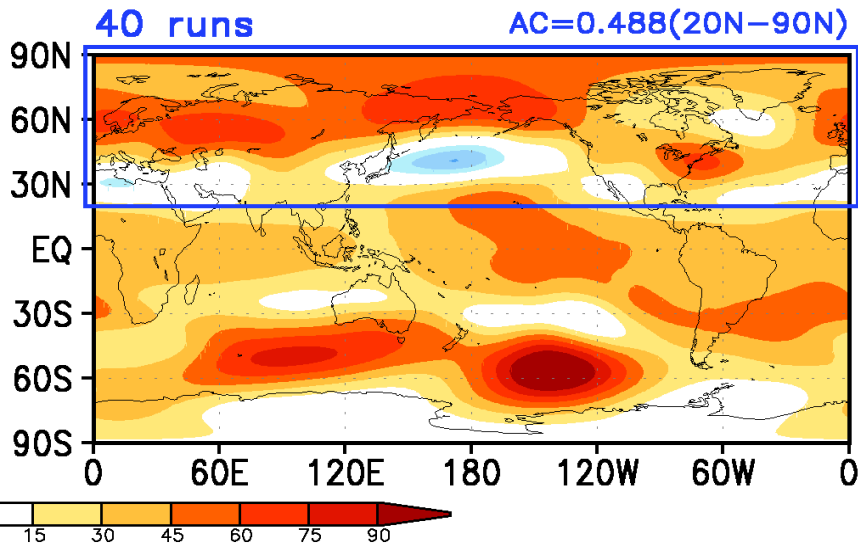
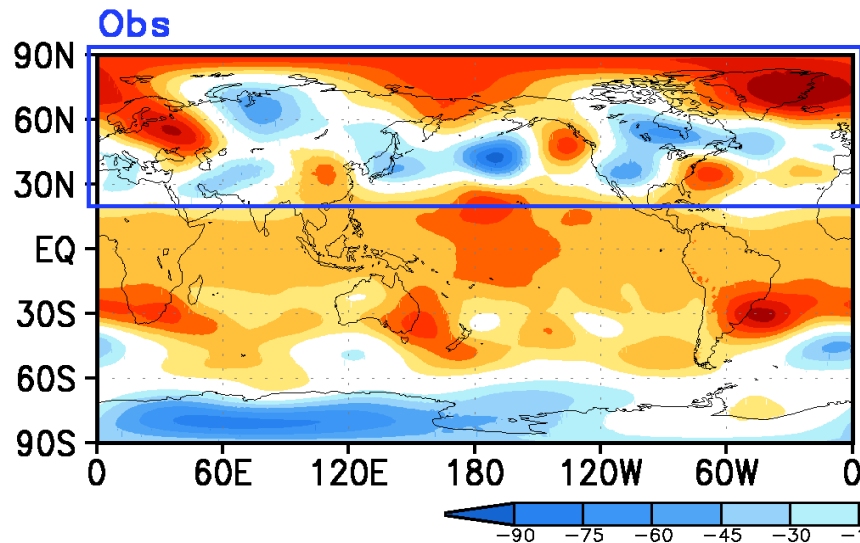
# AMJ2019 Anomaly Correlation for Individual CFSv2 Forecast with Observation --- z200 (20N–90N)



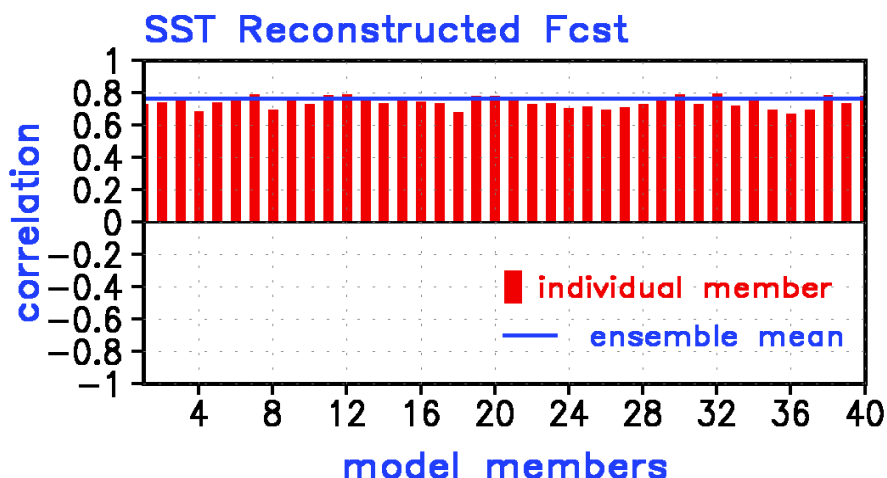
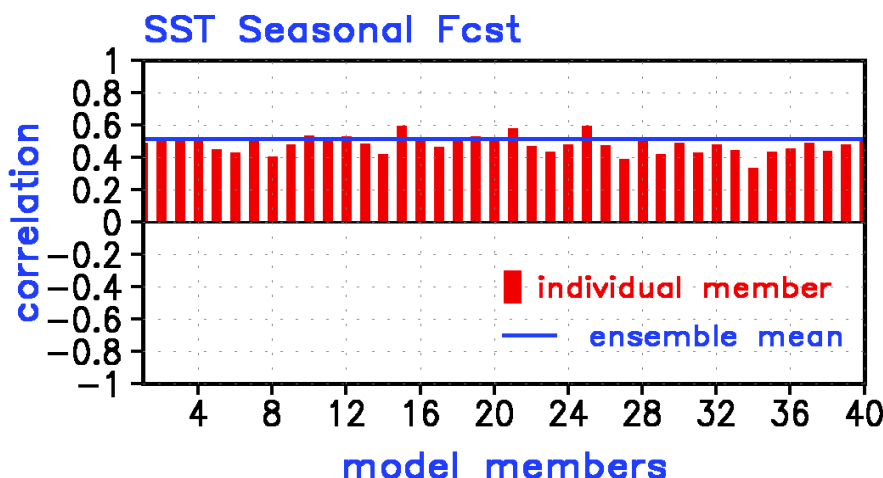
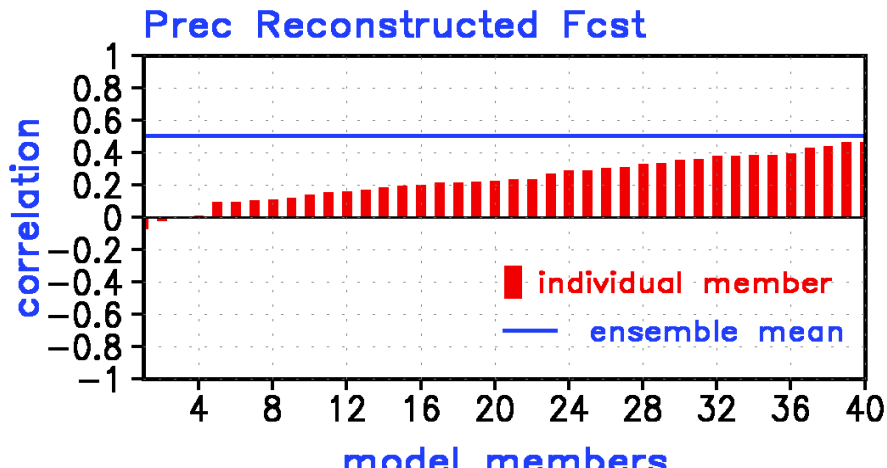
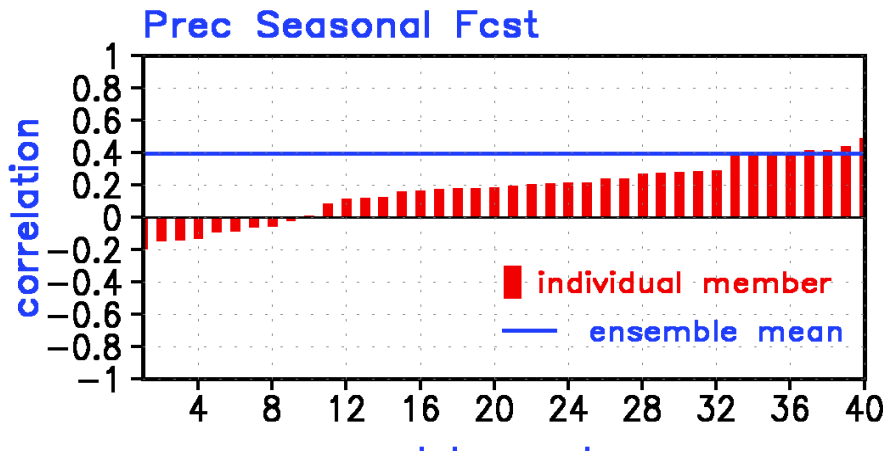
Observed & CFSv2 Forecast Ensemble Average Anomalies  
AMJ2019 z200(m) 40 runs/worst 4 runs/best 4 runs  
Seasonal Forecast



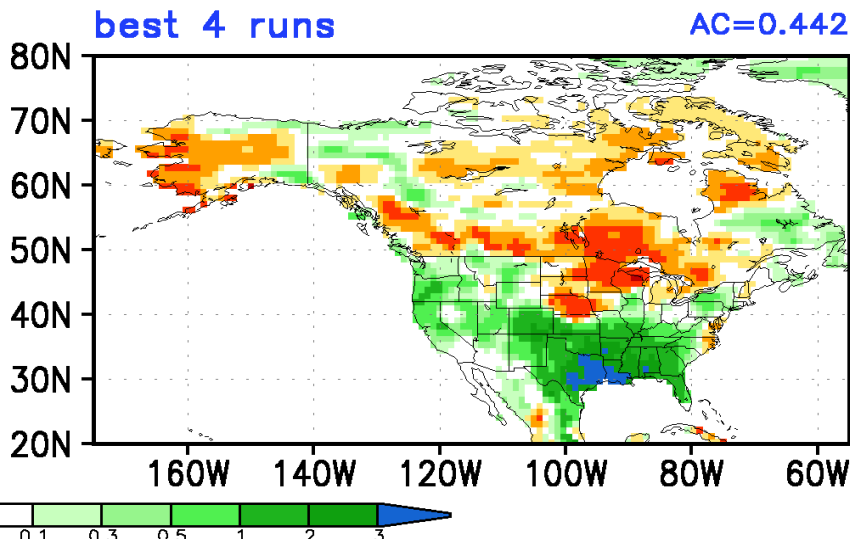
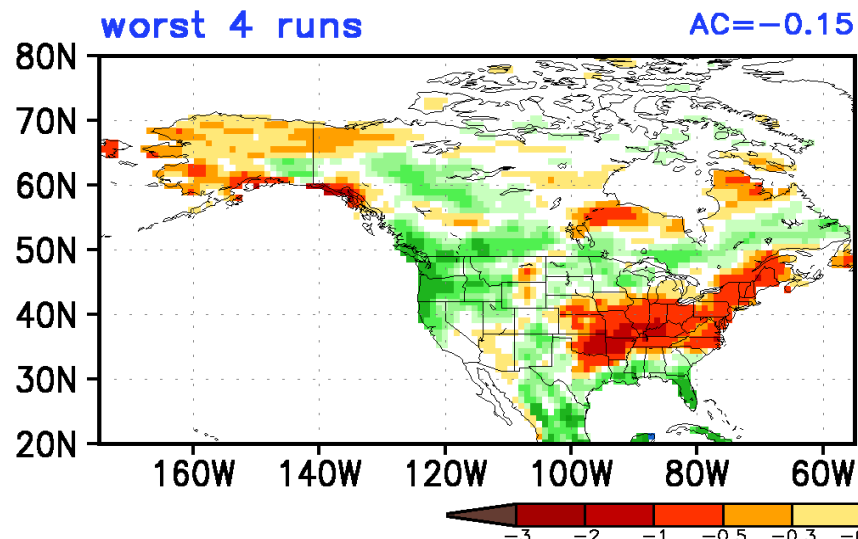
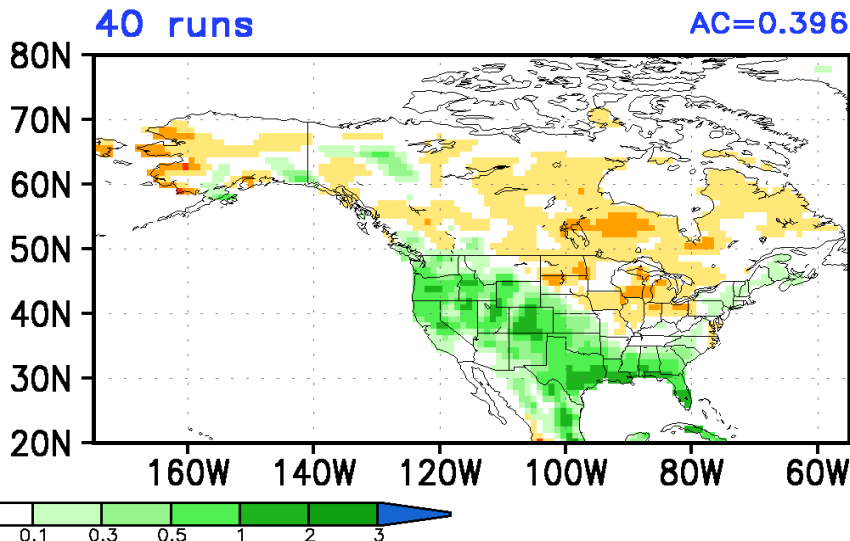
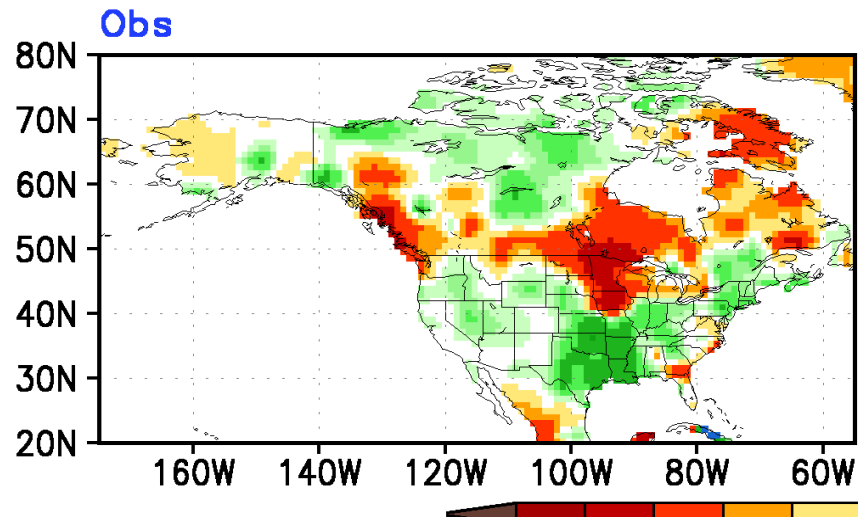
Observed & CFSv2 Forecast Ensemble Average Anomalies  
AMJ2019 z200(m) 40 runs/worst 4 runs/best 4 runs  
Reconstructed Forecast



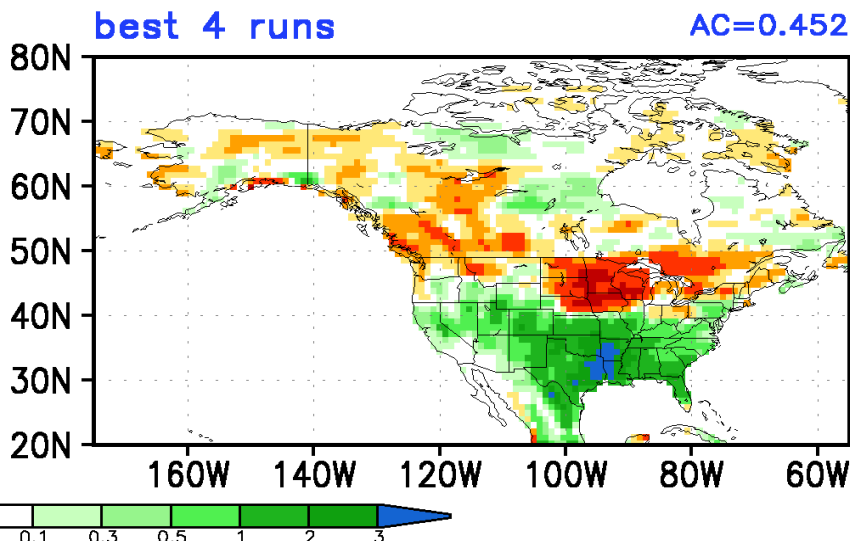
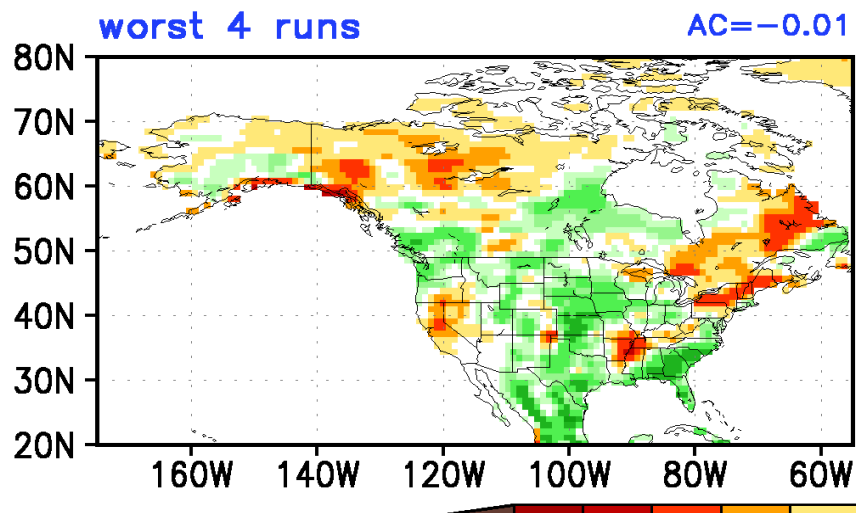
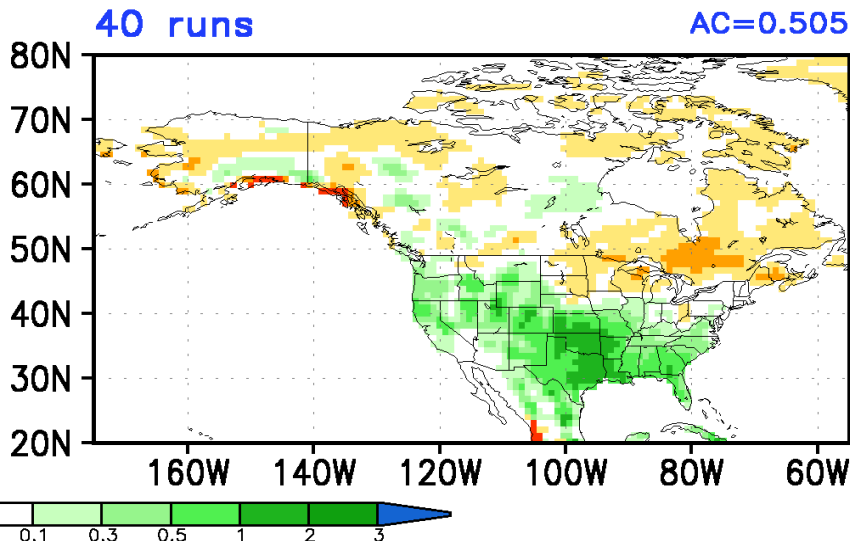
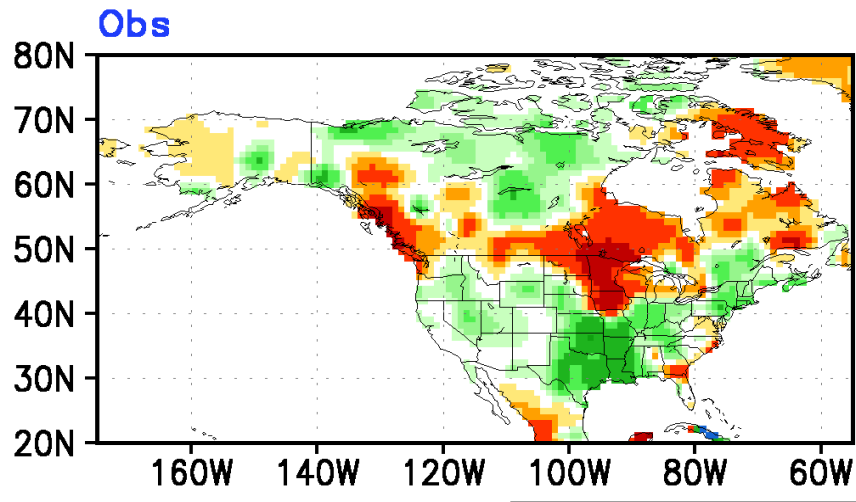
# AMJ2019 Anomaly Correlation for Individual CFSv2 Forecast with Observation -- Prec(NA)/SST(30S–30N)



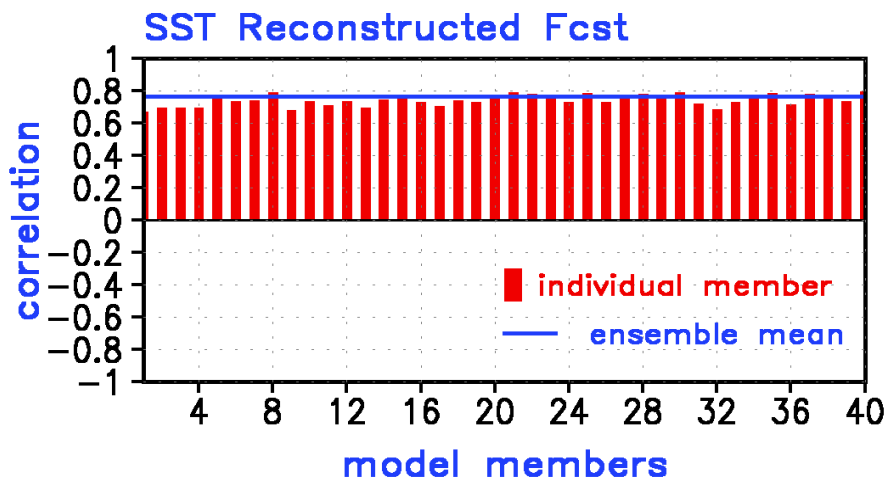
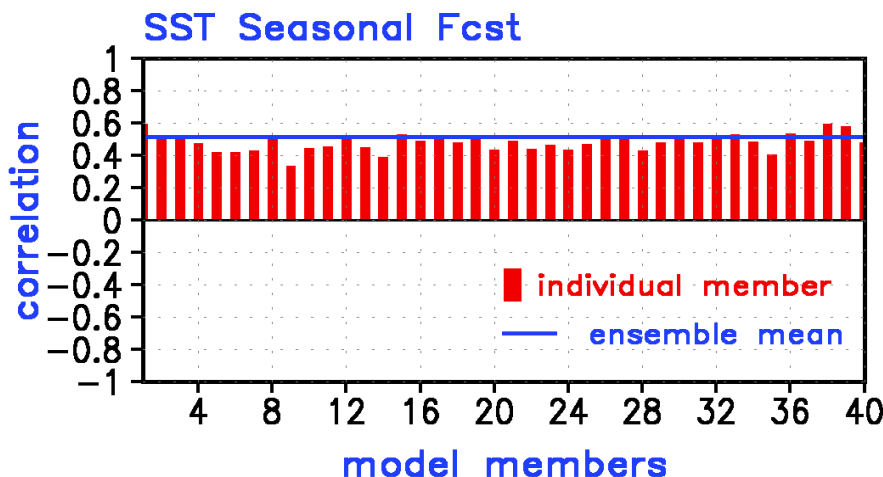
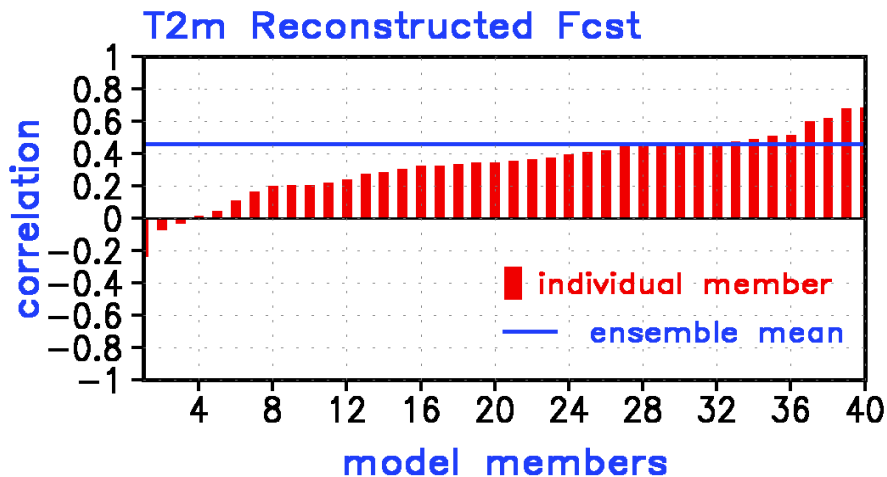
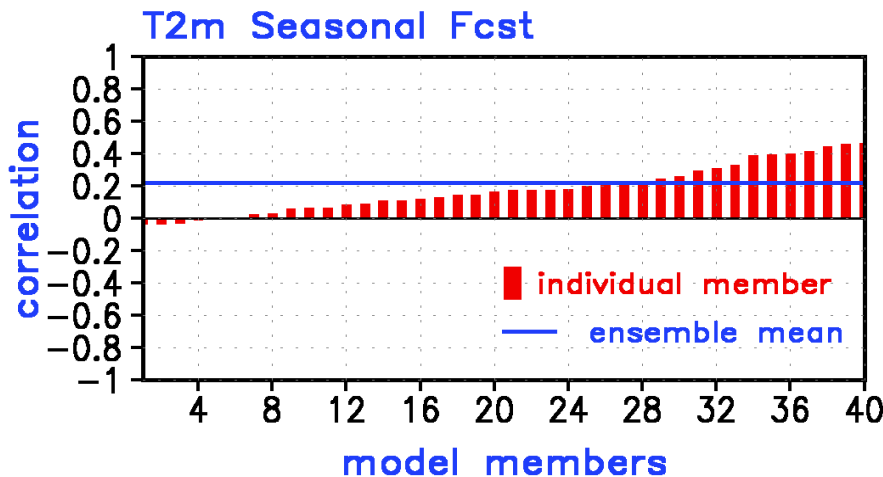
Observed & CFSv2 Forecast Ensemble Average Anomalies  
AMJ2019 Prec(mm/day) 40 runs/worst 4 runs/best 4 runs  
Seasonal Forecast



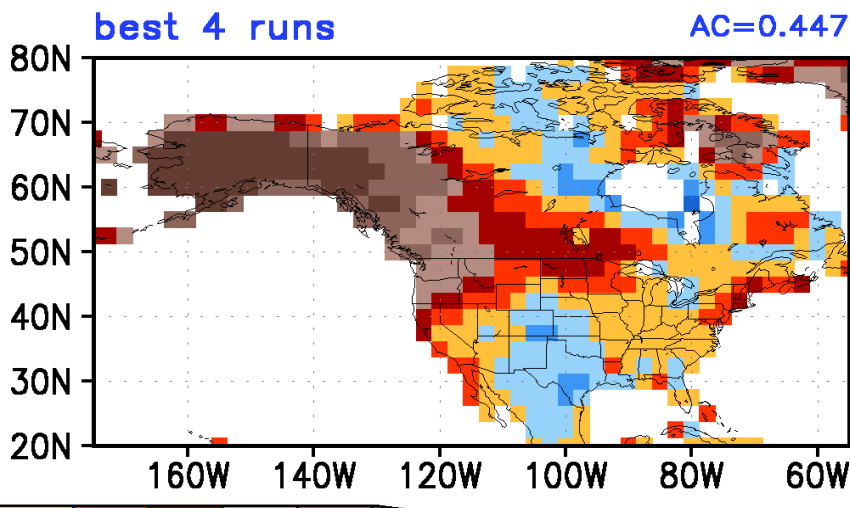
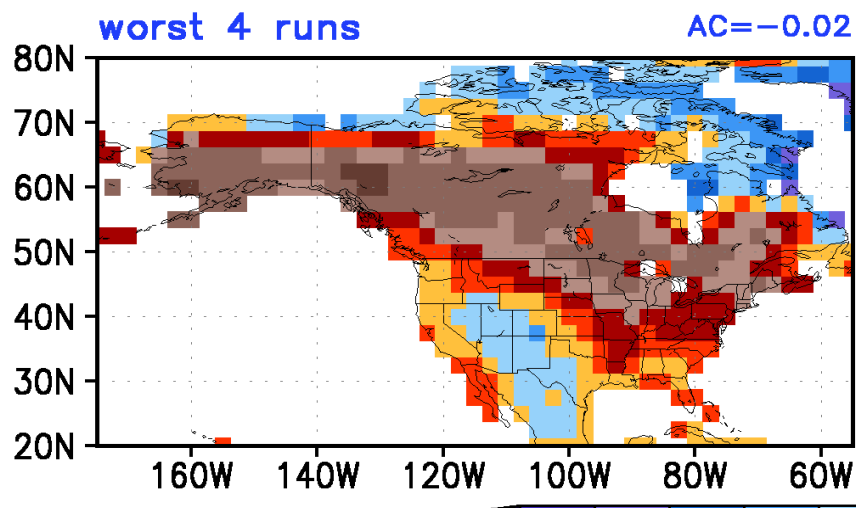
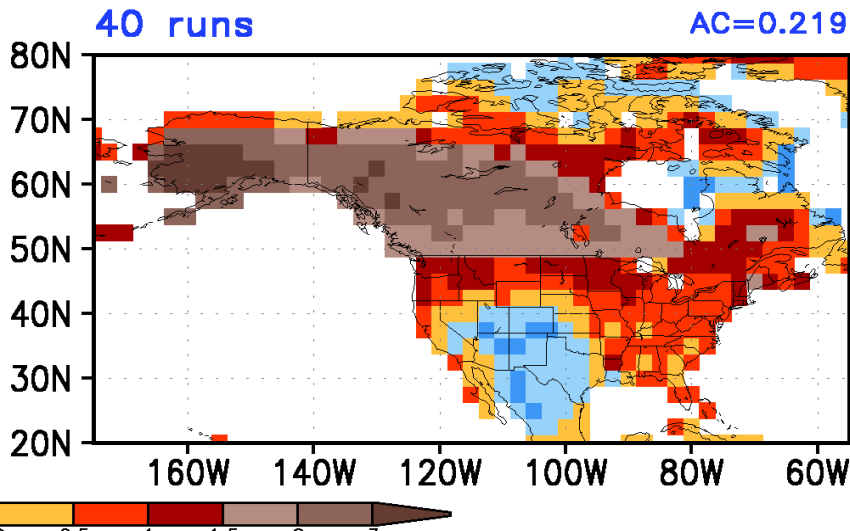
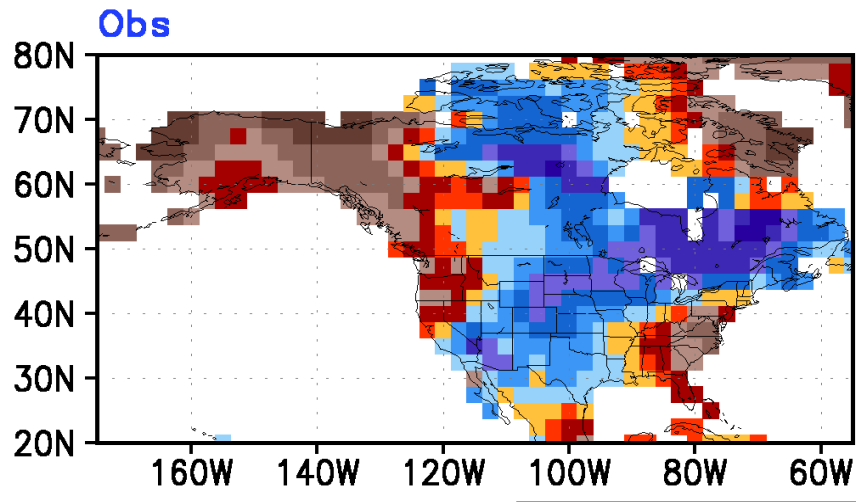
Observed & CFSv2 Forecast Ensemble Average Anomalies  
AMJ2019 Prec(mm/day) 40 runs/worst 4 runs/best 4 runs  
Reconstructed Forecast



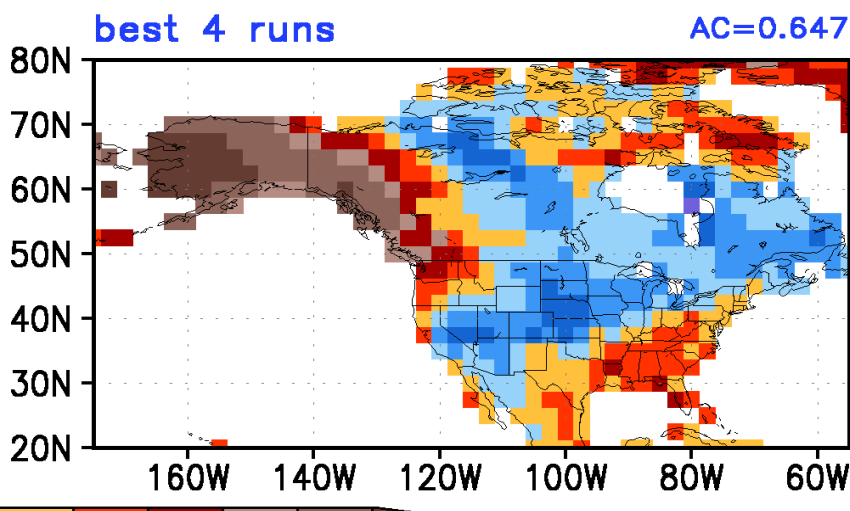
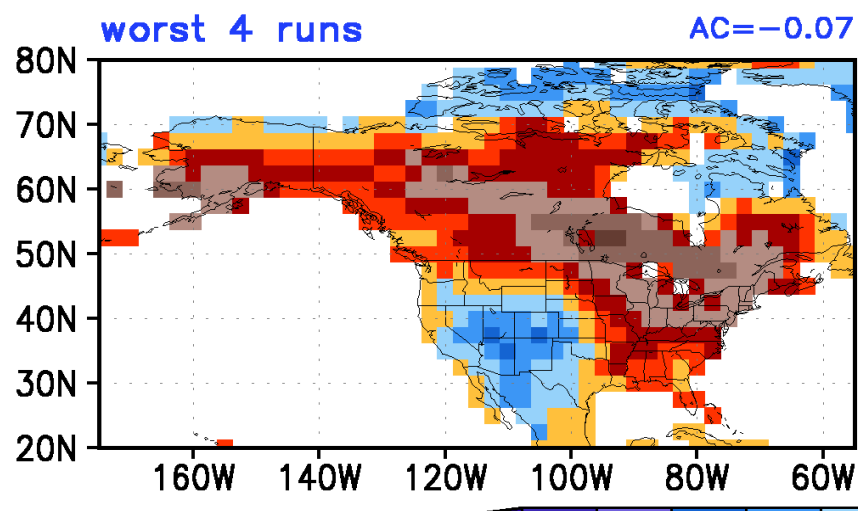
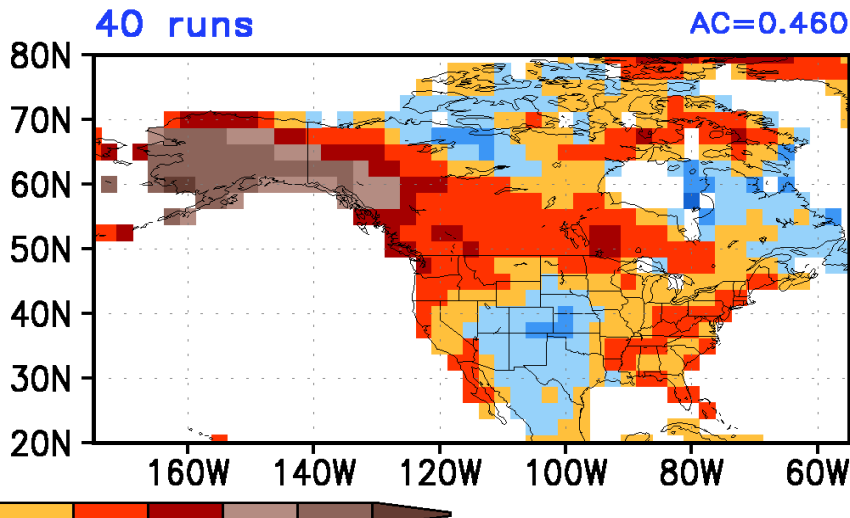
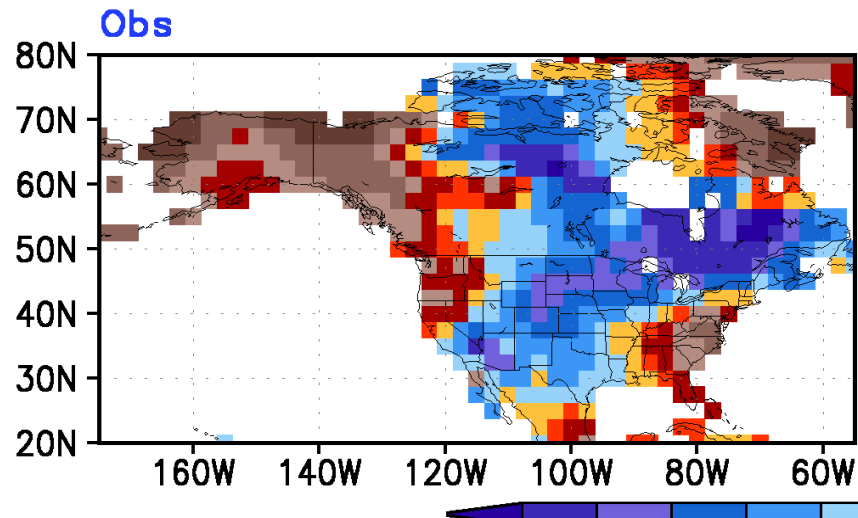
# AMJ2019 Anomaly Correlation for Individual CFSv2 Forecast with Observation -- T2m(NA)/SST(30S–30N)



Observed & CFSv2 Forecast Ensemble Average Anomalies  
AMJ2019 T2m(K) 40 runs/worst 4 runs/best 4 runs  
Seasonal Forecast

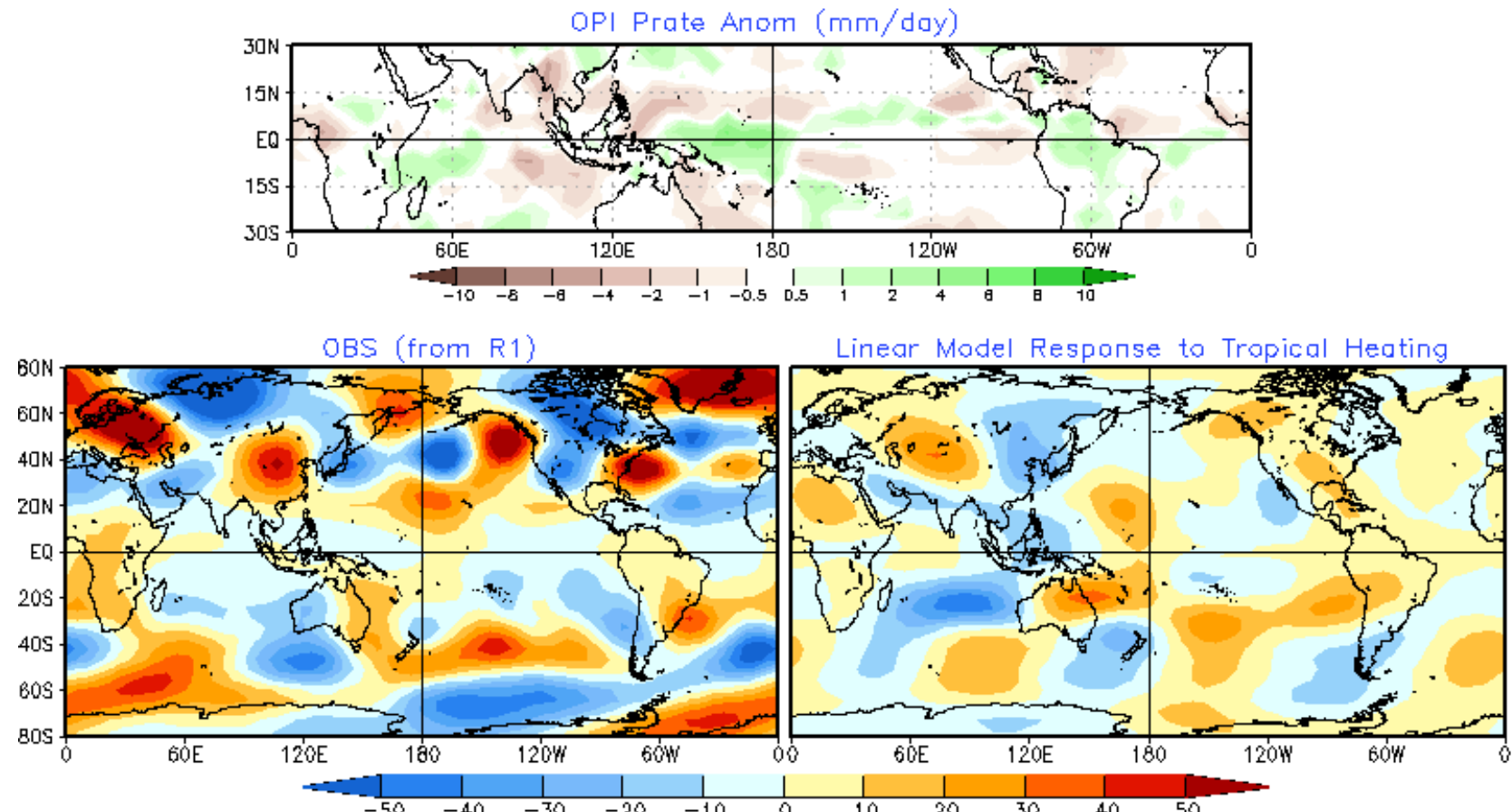


Observed & CFSv2 Forecast Ensemble Average Anomalies  
AMJ2019 T2m(K) 40 runs/worst 4 runs/best 4 runs  
Reconstructed Forecast



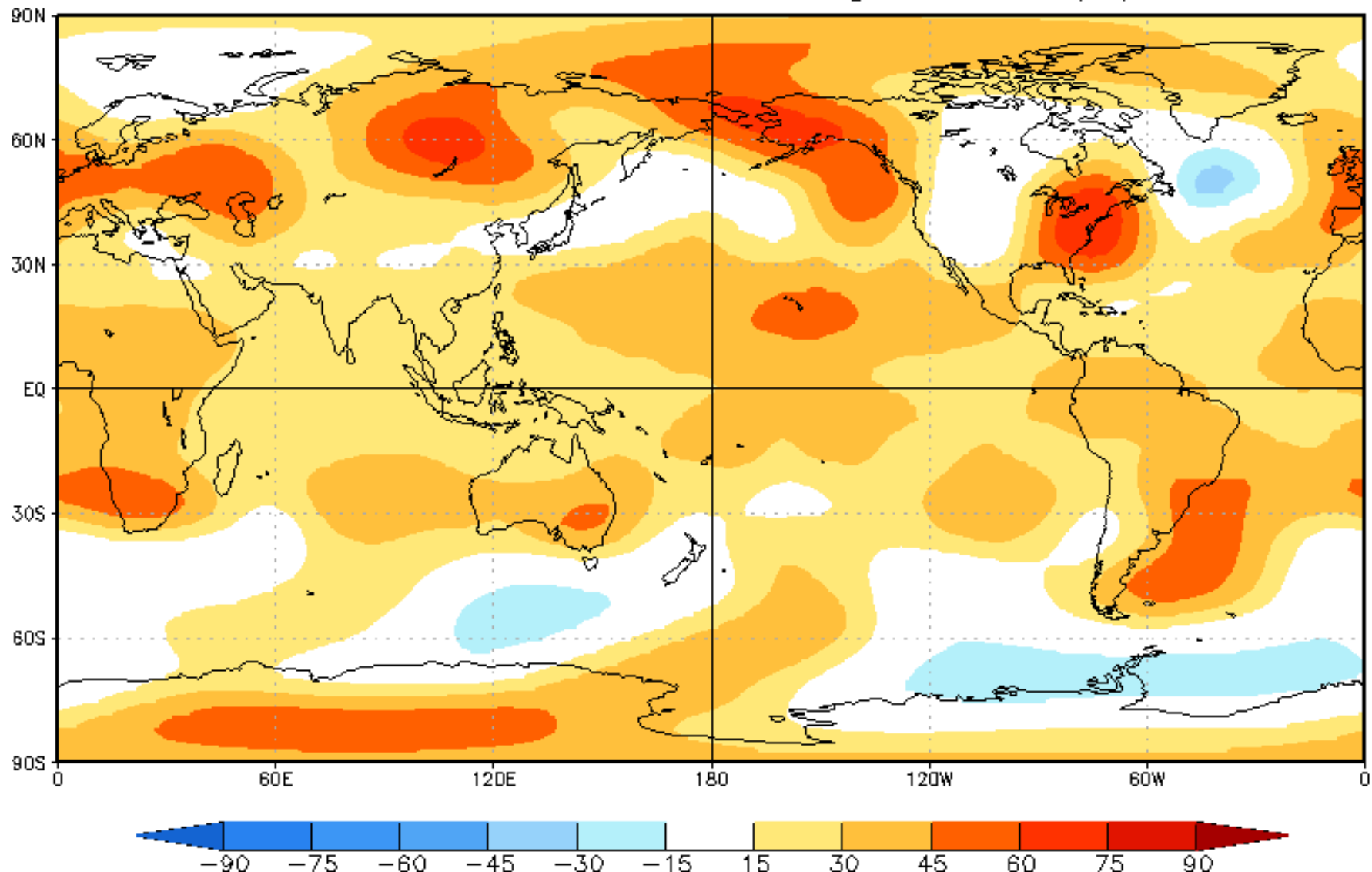
# 200mb Height from Linear Model

AMJ2019 200mb Eddy HGT(m)  
OBS vs. Linear Model Response to Tropical Heating  
Heating is converted from Prate in 15S–15N

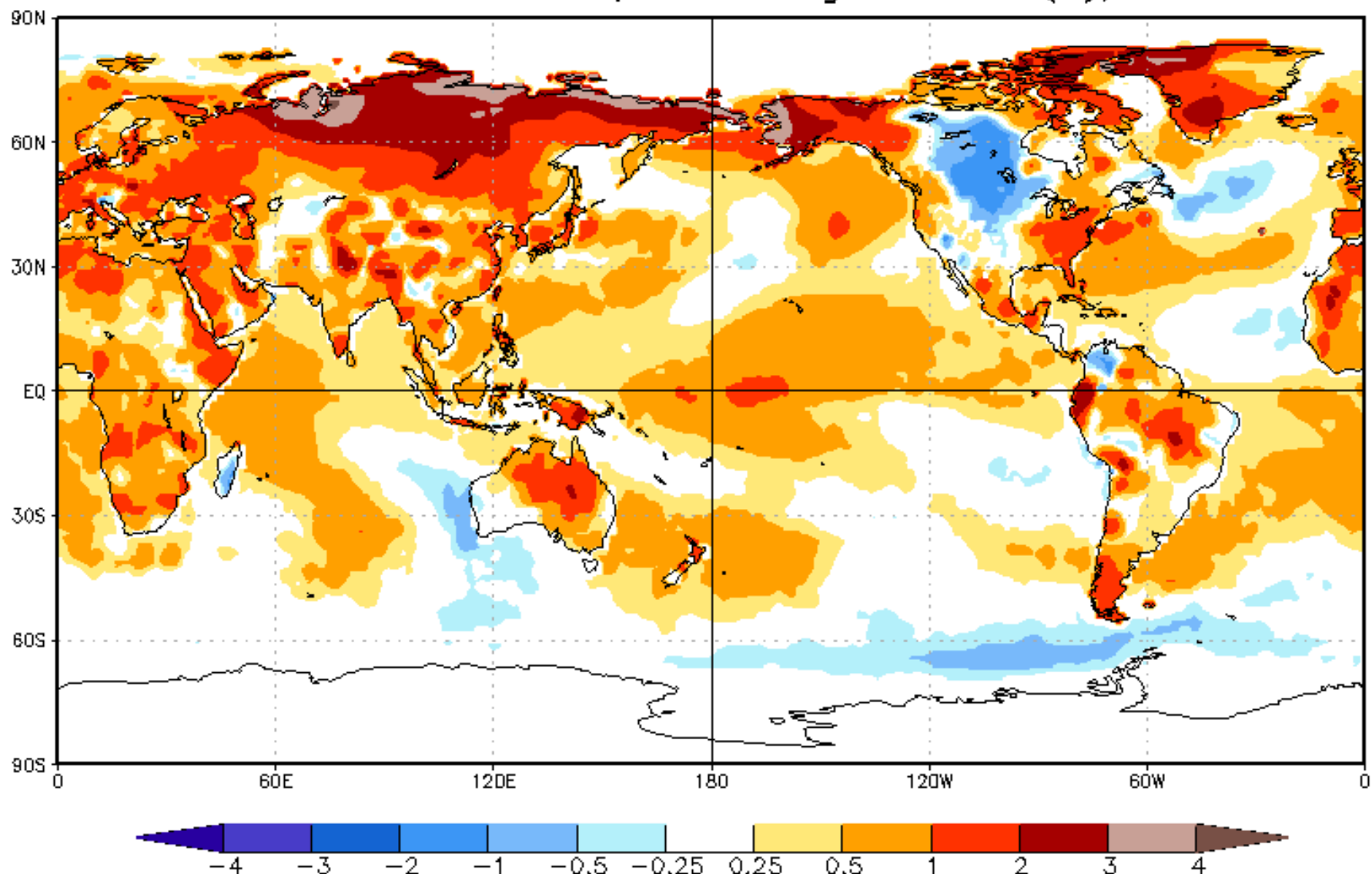


# Seasonal Forecasts from the Constructed Analog Model

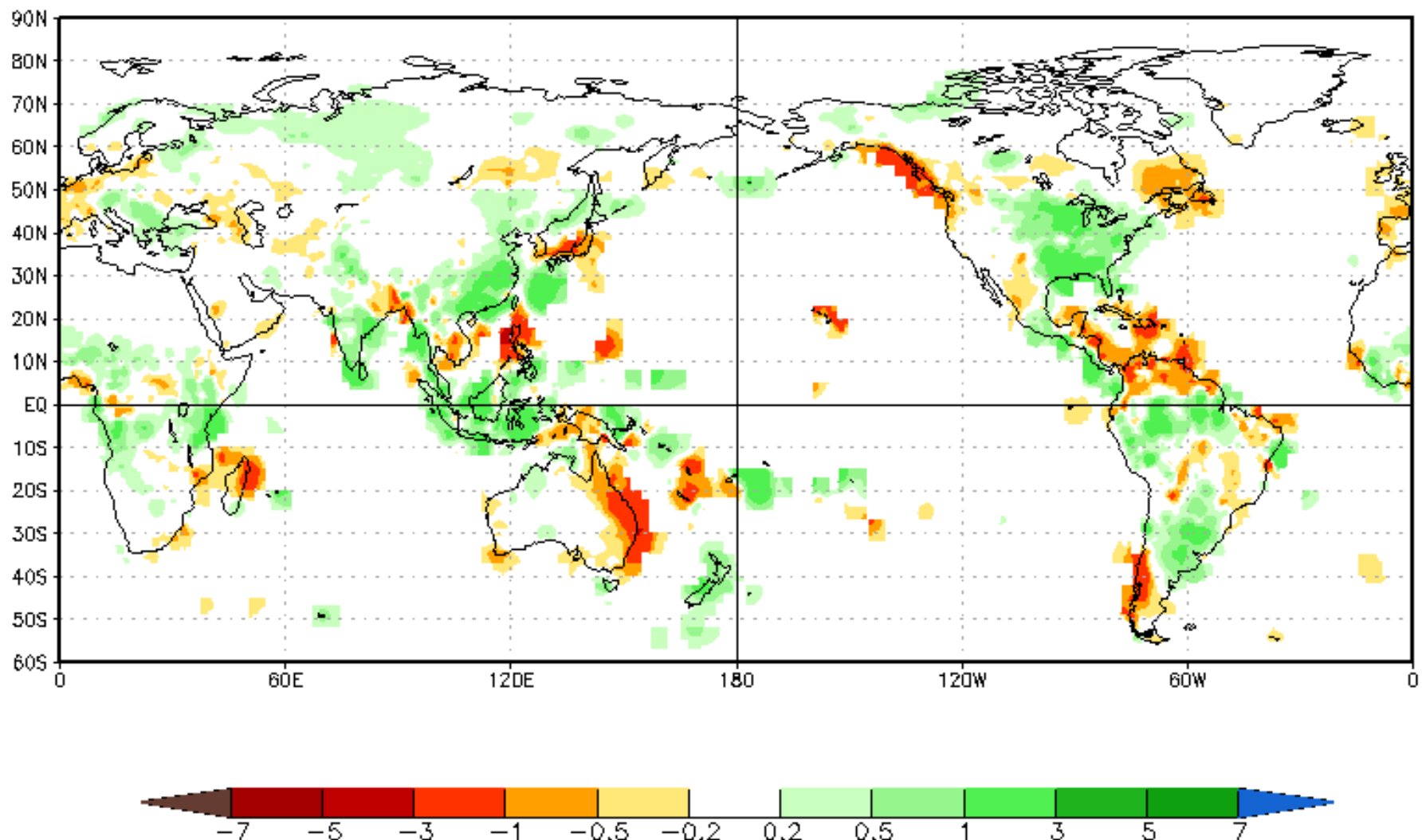
# CA HGT200 Prd for AMJ2019, ICs through Jun2019(m), Lead -3



CA T2m Prd for AMJ2019, ICs through Jun2019(K), Lead -3



# CA Prec Prd for AMJ2019, ICs through Jun2019(mm/day), Lead -3



# Seasonal Forecasts from WMO Lead Center for Long-Range Forecast Multi-Model Ensemble (LC-LRFMME)

<https://www.wmolk.org/>

- LC-LRFMME seasonal forecast are based on forecasts provided by WMO recognized Global Producing Centers (GPCs) for Long-Range Forecasts to the LC-LRFMME. Contribution of all GPCs is acknowledged.
- Seasonal forecasts from GPCs are merged into a multi-model ensemble forecast.
- LC-LRFMME forecasts are based on GPC seasonal forecast systems run during the first week of the month for the next season. For example, forecasts runs in first week of January for the seasonal mean of February-March-April.
- Forecasts in slides 42-45 are from the Lead Center.
- For latest seasonal outlook guidance see  
<http://www.wmo.int/pages/prog/wcp/wcasp/LC-LRFMME/index.php>
- *For more information see visit Lead Center website; also see Graham, R., and Co-authors, 2011: New perspectives for GPCs, their role in the GFCS and a proposed contribution to a 'World Climate Watch'. Climate Research, 47, 47-55.*

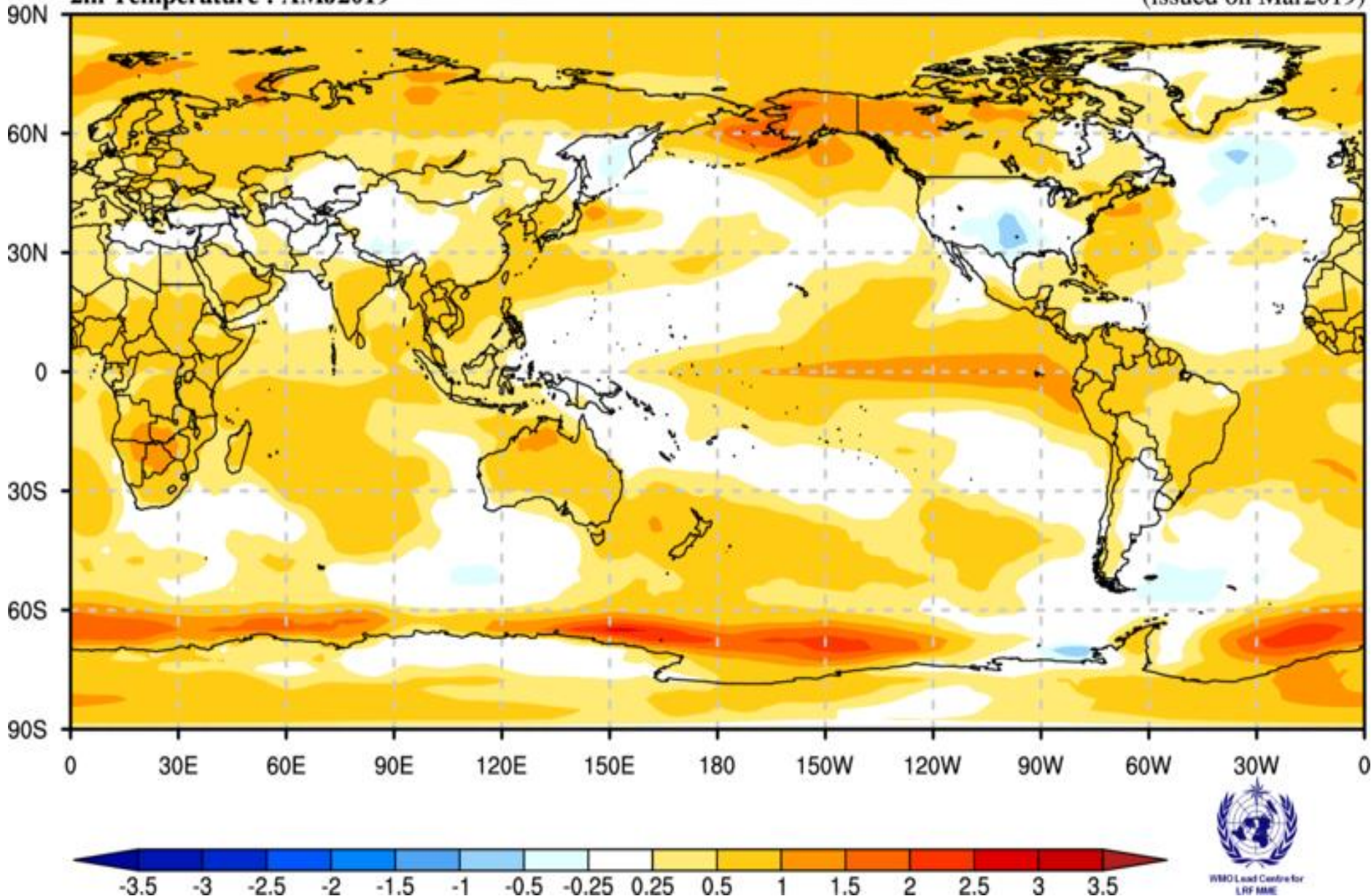
# Simple Composite Map

Beijing,CPTEC,Exeter,Melbourne,Montreal,Moscow,Offenbach,Pretoria,Seoul,Tokyo,Toulouse,Washington

[Unit : K]

2m Temperature : AMJ2019

(issued on Mar2019)



WMO Lead Centre  
LRF MME

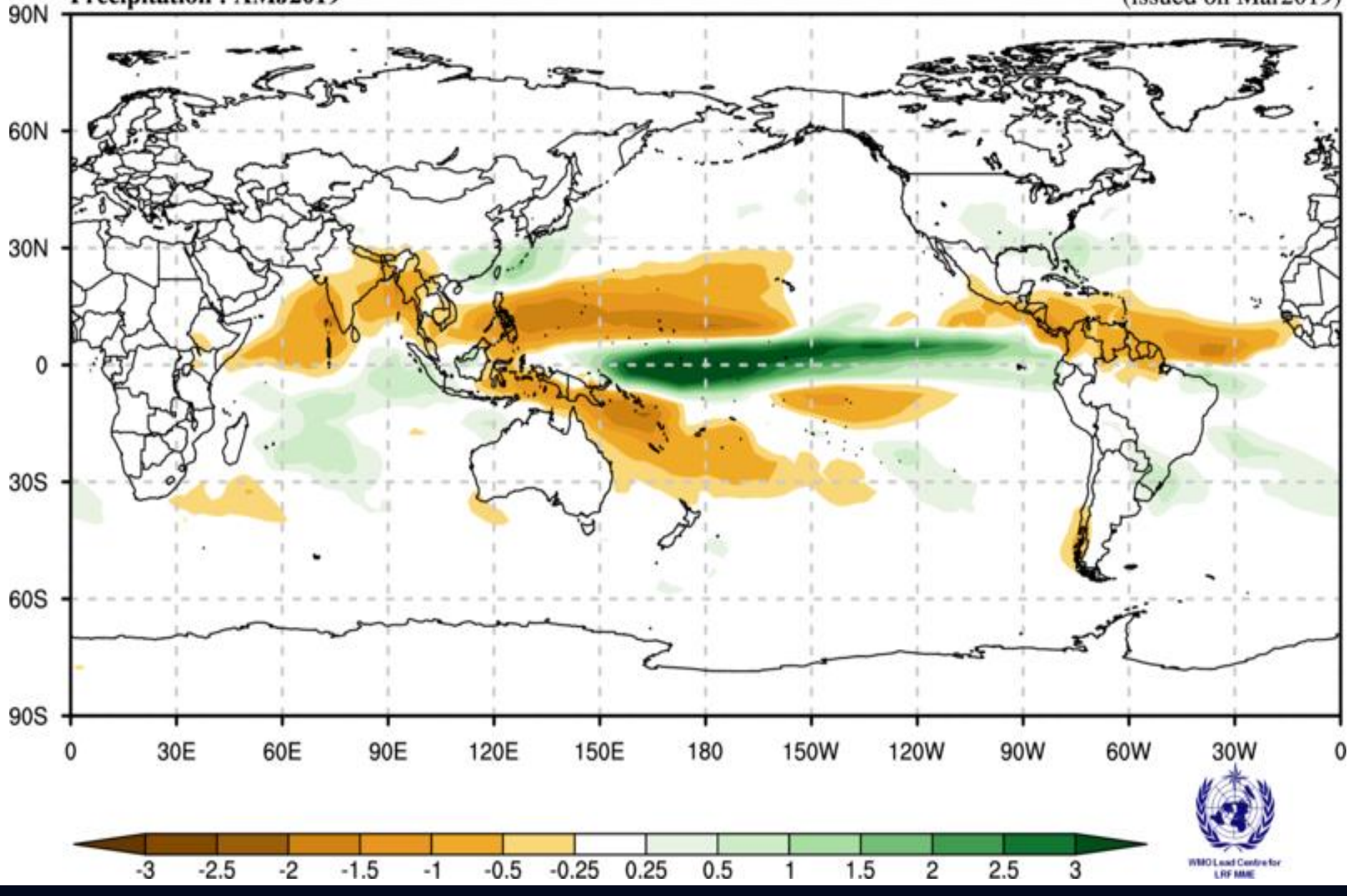
# Simple Composite Map

Beijing,CPTEC,Exeter,Melbourne,Montreal,Moscow,Offenbach,Pretoria,Seoul,Tokyo,Toulouse,Washington

[Unit : mm]

Precipitation : AMJ2019

(issued on Mar2019)



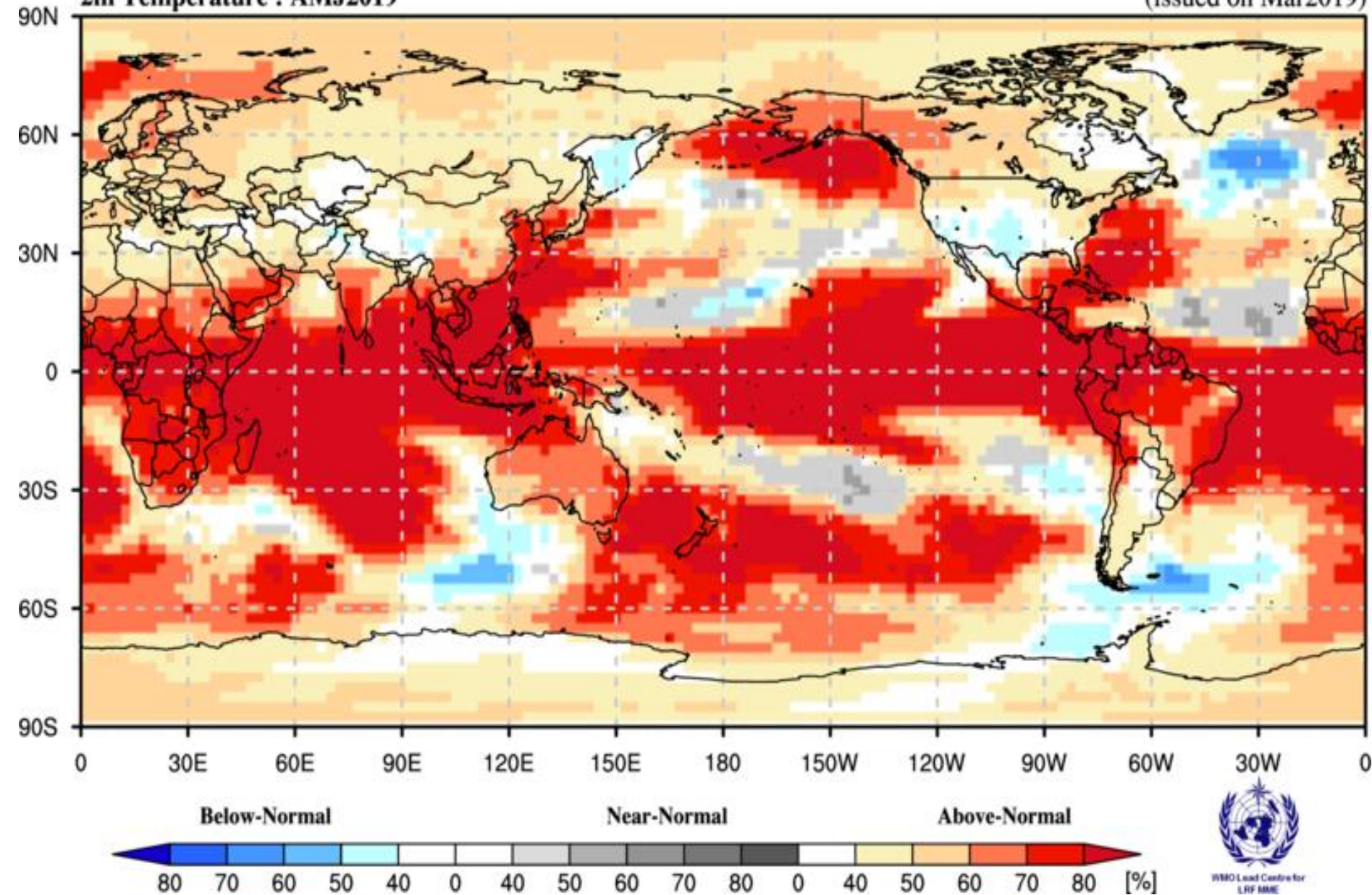
WMO Lead Center for  
LRF MME

# Probabilistic Multi-Model Ensemble Forecast

Beijing,CPTEC,ECMWF,Exeter,Melbourne,Montreal,Moscow,Offenbach,Pretoria,Seoul,Tokyo,Toulouse,Washington

2m Temperature : AMJ2019

(issued on Mar2019)

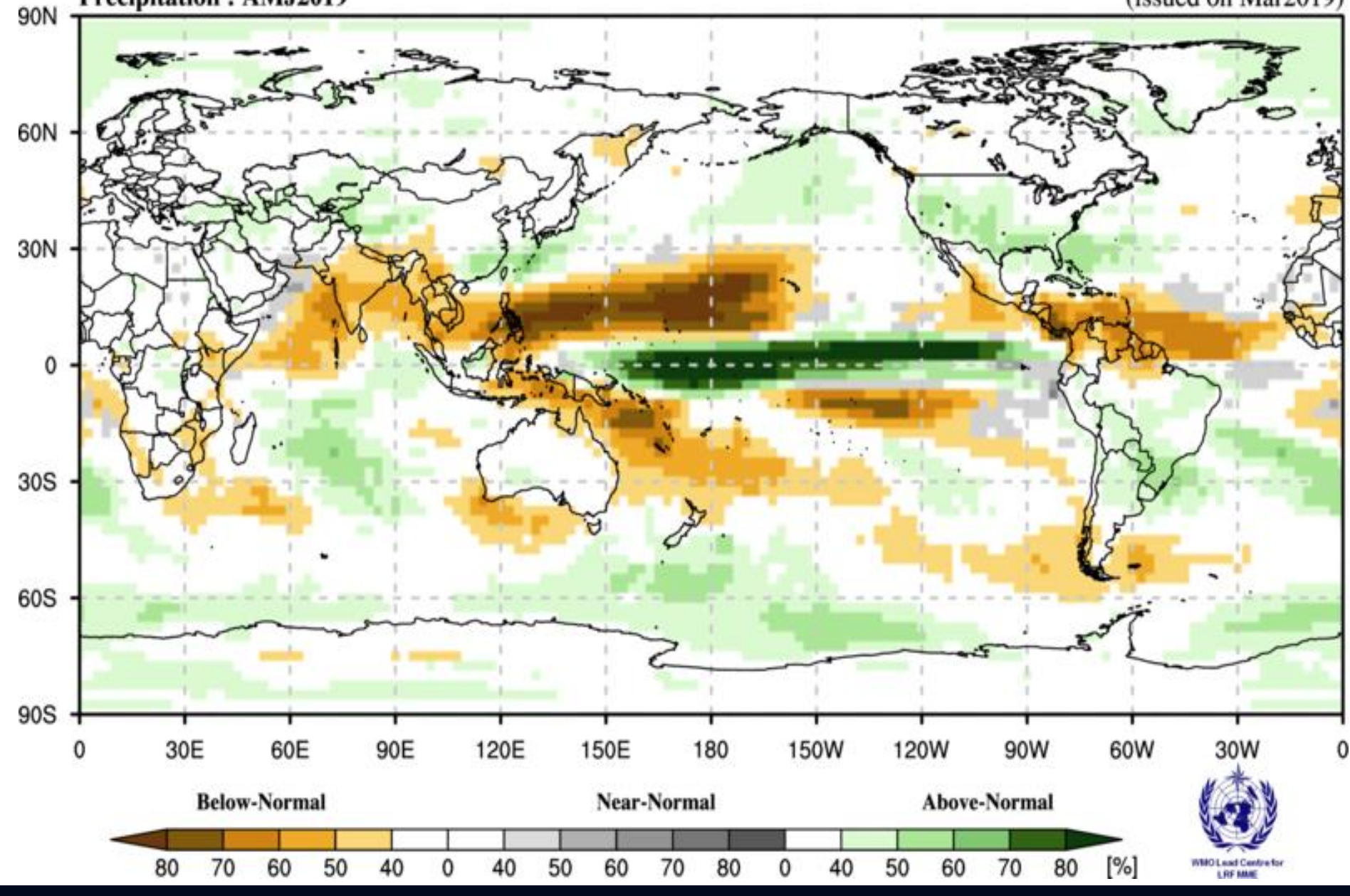


# Probabilistic Multi-Model Ensemble Forecast

Beijing,CPTEC,ECMWF,Exeter,Melbourne,Montreal,Moscow,Offenbach,Pretoria,Seoul,Tokyo,Toulouse,Washington

Precipitation : AMJ2019

(issued on Mar2019)



WMO Lead Centre  
for  
LRF MME

# References

- Fan, Y., and Dool H. van den Dool (2008), A global monthly land surface air temperature analysis for 1948-present. *J. Geophys. Res.*, 113, D01103. [doi:10.1029/2007JD008470](https://doi.org/10.1029/2007JD008470).
- Kumar, A., M. Chen, M. Hoerling, and J. Eischeid (2013), Do extreme climate events require extreme forcings? *Geophys. Res. Lett.*, 40, 3440-3445. [doi:10.1002/grl.50657](https://doi.org/10.1002/grl.50657).
- Reynolds, R. W. et al (2007), Daily high resolution-blended analyses for sea surface temperature. *J. Clim.*, 20, 5473-5496. [doi:10.1175/2007JCLI1824.1](https://doi.org/10.1175/2007JCLI1824.1).
- Saha, S. et al (2010), The NCEP climate forecast system reanalysis. *Bull. Amer. Meteor. Soc.*, 91, 1015-1057. [doi:10.1175/2010BAMS3001.1](https://doi.org/10.1175/2010BAMS3001.1).
- Saha, S. et al (2014), The NCEP climate forecast system version 2. *J. Clim.*, 27, 2185-2208. [doi:10.1175/JCLI-D-12-00823.1](https://doi.org/10.1175/JCLI-D-12-00823.1).
- Xie, P, and P. A. Arkin (1997), Global precipitation: A 17-year monthly analysis based on gauge observations, satellite estimates, and numerical model outputs. *Bull. Amer. Meteor. Soc.*, 78, 2539-2558. doi: [http://dx.doi.org/10.1175/1520-0477\(1997\)078%3C2539:GPAYMA%3E2.0.CO;2](http://dx.doi.org/10.1175/1520-0477(1997)078%3C2539:GPAYMA%3E2.0.CO;2)